HHS Public Access
Author manuscript
*Immunity*. Author manuscript; available in PMC 2019 November 20.

Published in final edited form as:
*Immunity*. 2018 November 20; 49(5): 886–898.e5. doi:10.1016/j.immuni.2018.09.004.

# RAS P21 Protein Activator 3 (RASA3) specifically promotes pathogenic T helper 17 cell generation by repressing T helper 2-biased programs

**Bing Wu**[1,2], **Song Zhang**[1,2], **Zengli Guo**[1,2], **Gang Wang**[1,2,3], **Ge Zhang**[1,2,4], **Ling Xie**[2,5], **Jitong Lou**[6], **Xian Chen**[2,5], **Di Wu**[6,7], **Wolfgang Bergmeier**[5], **Junnian Zheng**[3,*], and **Yisong Y. Wan**[1,2,8,*]

[1]Lineberger Comprehensive Cancer Center, School of Medicine, University of North Carolina at Chapel Hill, NC, 27599, USA

[2]Department of Microbiology and Immunology, School of Medicine, University of North Carolina at Chapel Hill, NC 27599, USA

[3]Jiangsu Center for the Collaboration and Innovation of Cancer Biotherapy, Cancer Institute, Xuzhou Medical University, Xuzhou, Jiangsu 221002, China

[4]Department of Immunology,Dalian Medical University,Dalian 116044, China

[5]Department of Biochemistry and Biophysics, School of Medicine, University of North Carolina at Chapel Hill, Chapel Hill, North Carolina, USA

[6]Department of Biostatistics, Gillings School of Global Public Health, University of North Carolina at Chapel Hill, Chapel Hill, North Carolina, USA

[7]Department of Periodontology, School of Dentistry, University of North Carolina at Chapel Hill, Chapel Hill, North Carolina, USA

## SUMMARY

Pathogenic-Th17 (pTh17) cells drive inflammation and immune-pathology, but whether pTh17 cells are a Th17-subset whose generation is under specific molecular control remains unaddressed. We found that Ras p21 protein activator 3 (RASA3) was highly expressed by pTh17 cells relative to non-pTh17 cells and was required specifically for pTh17 generation *in vitro* and *in vivo*. Mice conditionally deficient for *Rasa3* in T cells showed less pathology during experimental

[*]Correspondence: wany@email.unc.edu (Y.W.), jnzheng@xzmc.edu.cn (J.Z.).
[8]Lead Contact.

AUTHOR CONTRIBUTIONS
B.W. contributed to the design and implementation of the cellular, molecular, biochemical and animal experiments and the writing of the manuscript; S.Z. contributed to the gene knockdown experiments; Z.G. contributed to the protein stability and ubiquitination experiments; G.W. and J.Z. contributed to RNA-seq experiments; X.L. and X.C. contributed to mass-spectrometry and data analysis. J.L. and D.W. contributed to bioinformatic analysis; G.Z. contributed to EAE experiments; W.B. contributed critical reagents; Y.Y.W. conceived the project, designed experiments and wrote the manuscript.



DECLARATION OF INTERETS
The authors declare no competing financial interests.

autoimmune encephalomyelitis. *Rasa3*-deficient T cells acquired a Th2-biased program that dominantly *trans*-suppressed pTh17 cell generation via interleukin 4 production. The Th2-bias of *Rasa3*-deficient T cells was due to aberrantly elevated transcription factor IRF4 expression. RASA3 promoted proteasome-mediated IRF4 protein degradation by facilitating interaction of IRF4 with E3-ubiquitin ligase Cbl-b. Therefore, a RASA3-IRF4-Cbl-b pathway specifically directs pTh17 cell generation by balancing reciprocal Th17-Th2 programs. These findings indicate that a distinct molecular program directs pTh17 generation and reveals targets for treating pTh17-related pathology and diseases.

## Graphical abstract

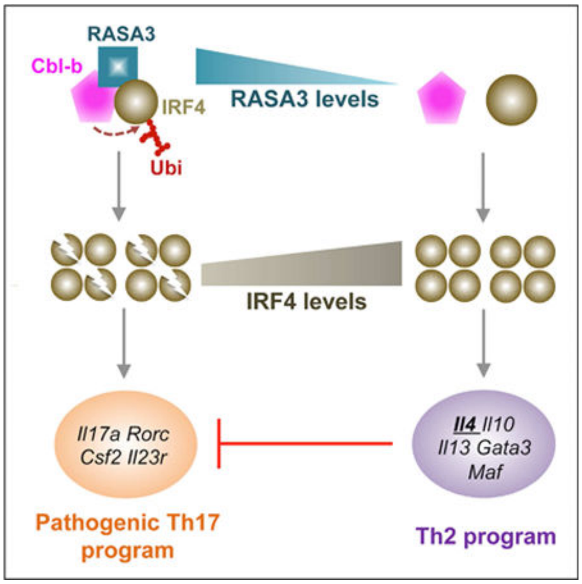


### Keywords

pathogenic Th17 cell; RASA3; EAE disease; pathogenic-Th17-Th2 reciprocal programs; IL-4; IRF4; Cbl-b

## INTRODUCTION

CD4$^+$ T cells differentiate into distinct effector T cell subsets to direct appropriate and effective responses to clear pathogens, eradicate tumors and maintain immune homeostasis. Conversely, aberrant effector CD4$^+$ cell function often leads to inflammatory and autoimmune diseases (Zhu et al., 2010). Since the proposition of helper T (Th) 1 and Th2 cell paradigm in the 1980's (Mosmann et al., 1986), additional Th cell types including Th17 (Harrington et al., 2005; Park et al., 2005) and regulatory T (Treg) cells (Sakaguchi, 2000) have been documented to function in distinct manners to control diverse and yet specific immune responses. In order to understand immune regulation during disease development and to treat immune-related diseases, we must address how the generation of Th cell subsets are controlled, a vital question that is under intensive investigation for decades.

Different transcription factors master distinct Th cell subsets. T-bet, GATA3, RORγt (RAR-related orphan receptor gamma) and Foxp3 are central to Th1, Th2, Th17 and Treg cell generation and function respectively (Fontenot et al., 2003; Hori et al., 2003; Ivanov et al., 2006; Szabo et al., 2000; Zheng and Flavell, 1997). Nonetheless, the molecular programs controlling various Th cells are unsegregated but rather overlapping. The shared underlying molecular networks enable the intricate functional relationships, antagonistic or synergistic, between different Th cell subsets. It is the distinct and yet over-lapping molecular programs dictate the development and function of discrete Th cell subsets (O'Shea and Paul, 2010).

Th17 cells that produce the signature cytokine interleukin 17 (IL-17) have attracted great and increasing attention since its discovery, for its broad and diverse function in controlling immune responses during infection, inflammation, autoimmunity and cancer (Dong, 2008; Korn et al., 2009; Patel and Kuchroo, 2015; Zou and Restifo, 2010). Varying combinations of cytokine signaling activated by transforming growth factor-β1 (TGF-β1), IL-6, IL-1β and IL-23 promotes RORγt expression and the subsequent Th17 cell development and function. Much of the current knowledge on the Th17-determining molecular program is obtained by studying TGF-β1+IL-6 induced vTh17 cells (Bettelli et al., 2006). TGF-β1+IL-6 induced Th17 cells, albeit can be pathogenic to certain degree, are largely non-pathogenic and produce signature immune regulatory cytokine IL-10 (McGeachy et al., 2007; Stumhofer et al., 2007). Similarly, *in vivo* generated Th17 cells can be both pathogenic and non-pathogenic in a context dependent manner (Ahern et al., 2010; Esplugues et al., 2011). These observations suggest that pathogenic and non-pathogenic-Th17 cells are functionally distinct and may be under specific molecular control (Bettelli et al., 2008; Peters et al., 2011). To support such a notion, studies demonstrated that Th17 cells need additional IL-23 signal to gain pathogenic function (Ahern et al., 2010; Ghoreschi et al., 2010; Langrish et al., 2005; McGeachy et al., 2009). Pathogenic-Th17 and non-pathogenic-Th17 cells have different gene expression profiles; pathogenic-Th17 cell specifically express high levels of GM-CSF, IL-23R and low levels of CD5L for pathogenicity (El-Behi et al., 2011; Lee et al., 2012; Wang et al., 2015). In addition, cytokine combination IL-1β+IL-6+IL23 is able to induce pathogenic-Th17 cells (Chung et al., 2009; Ghoreschi et al., 2010; Lee et al., 2012; Wang et al., 2015). Therefore, the acquisition of pathogenicity of Th17 cells requires special molecular programs.

Nevertheless, the intriguing possibility remaining unaddressed and thus under intense pursuit is whether pathogenic and non-pathogenic-Th17 cells can be categorized as distinct Th17 subtypes whose generation is controlled by discrete molecular programs. Available evidences suggest the contrary however, because currently identified factors vcritical for Th17 cell differentiation including RORγt, BATF and IRF4 (interferon regulatory factor 4) are indistinguishably required for the generation of both pathogenic-and non-pathogenic-Th17 cells (Brustle et al., 2007; Ivanov et al., 2006; Schraml et al., 2009).

Here, we revealed that Ras p21 protein activator 3 (RASA3), a GTPase activating protein of GAP1 sub-family (Schurmans et al., 2015), is specifically required for the generation of pathogenic Th17 cells. RASA3 does so by balancing the reciprocal molecular programs of pTh17-Th2 cells via RASA3-IRF4-Cbl-b (Cbl proto-oncogene-B) pathway. The study provides evidences to support the notion that pathogenic and non-pathogenic-Th17 cells are distinct Th17 subtypes generated through discrete molecular programs. In addition, it reveals RASA3-IRF4-Cbl-b a critical molecular hub to direct pathogenic-Th17 cell generation; targeting this hub may benefit the treatment of Th17 cell-related pathology and diseases.

## RESULTS

### RASA3 is required specifically for pathogenic-Th17 (pTh17) cell generation *in vitro*.

To identify the molecule(s) that determine pTh17 cell generation, we compared the gene expression between IL-6+IL-1β+IL-23-polarized pTh17 cells and IL-6+TGF-β1-polarized Th17 cells that are much less pathogenic. We found that RASA3, a factor previously identified as being highly expressed by Th17 cells (Lee et al., 2012), was preferentially upregulated at both mRNA (Figure 1a) and protein (Figure 1b) levels during pTh17 cell differentiation, suggesting its potential role in pTh17 cells. RASA3 has been well studied for platelet function (Stefanini et al., 2015). Its role in T cells however remains unknown.

To investigate RASA3 function in T cells, we generated *Rasa3*$^{flox/flox}$*Cd4Cre* mice, where RASA3 is specifically deleted in T cells. *Rasa3*$^{flox/flox}$*Cd4Cre* mice were born at the Mendelian ratio and grossly normal. The thymic development and peripheral Maintenanceof T cells in *Rasa3*$^{flox/flox}$*Cd4Cre* mice were comparable to *Rasa3*$^{flox/+}$*Cd4Cre* mice (Figure S1a). The T cell homeostasis in the periphery (Figure S1b, S1c, S1d, S1e) and intestines (Figure S1f) remained unperturbed in the absence of RASA3. The normal phenotype of RASA3-deficient T cells under steady state allowed us to investigate how RASA3 controls Th17 cell differentiation.

When activated in the presence of IL-6+TGF-β1, RASA3-deficient and –sufficient CD4$^+$ T cells generated similar percentages of IL-17A$^+$ cells (Figure 1c). In addition, compared to RASA3-sufficient CD4$^+$ T cells, RASA3-deficient CD4$^+$ T cells expressed largely normal levels of *Il17a*, *Rorc, Il23r* and *Csf2*, but higher levels of *Il10* and *Cd5l* (Figure 1d). Nonetheless, when activated in the presence of IL-1β+IL-6+IL-23, RASA3-deficient cells generated much lower percentages of IL-17A$^+$ cells than RASA3-suffícent cells (Figure 1e), with impaired expression of pTh17-related genes, including *Il17a, Rorc, Il23r* and *Csf2*. The expression of *Il10* and *Cd5l*, signature genes for non-pathogenic-Th17 cells, was however elevated in RASA3-deficient pTh17 cells (Figure 1f). The differential requirement of RASA3 for pTh17 cell generation was not due to a difference in T cell proliferation or survival. RASA3-deficient and -sufficient CD4$^+$ T cells proliferated (Figure 1g) and survived (Figure 1h) similarly when activated in the presence of IL-1β+IL-6+IL-23 or IL-6+TGF-β1. In addition, the Th1 and Th2 cell differentiation appeared normal in the absence of RASA3 (Figure S1g). These findings therefore suggest that the generation of pTh17 cells specifically requires RASA3.

### RASA3 is required for pTh17 cell generation and immune-pathology during Experimental Autoimmune Encephalomyelitis (EAE)

The generation of pTh17 cells is paramount to induce tissue immune-pathology for the development of autoimmune diseases including Experimental Autoimmune Encephalomyelitis (EAE), a mouse model for multiple sclerosis. The aforementioned findings promoted us to investigate whether RASA3 is required for pTh17 cell generation and immune-pathology *in vivo* during myelin oligodendrocyte glycoprotein (MOG) and complete freund's adjuvant (CFA) elicited EAE. We found that the incidence of EAEdisease was lower and the disease onset was delayed in *Rasa3*$^{flox/flox}$*Cd4Cre* mice when compared to *Rasa3*$^{flox/+}$*Cd4Cre* mice (Figure 2a). In addition, the EAE was less severe in *Rasa3*$^{flox/flox}$*Cd4Cre* mice, because the EAE clinic scores of *Rasa3*$^{flox/flox}$*Cd4Cre* mice were lower than those of *Rasa3*$^{flox/+}$*Cd4Cre* mice (Figure 2b). Consistently, the tissue immune-pathology of the spinal cord was much milder in *Rasa3*$^{flox/flox}$*Cd4Cre* mice than in *Rasa3*$^{flox/+}$*Cd4Cre* mice (Figure 2c).

Further immunological analysis revealed that there were fewer spinal cord-infiltrating IL-17A$^+$ CD4$^+$ T cells in *Rasa3*$^{flox/flox}$*Cd4Cre* mice than in *Rasa3*$^{flox/+}$*Cd4Cre* mice (Figure 2d, e), although the numbers of spinal cord infiltrating CD4$^+$ cells were similar between these two types of mice (Figure S2a). On the contrary, the fractions of IL-10$^+$ cells were increased in spinal cord-infiltrating CD4$^+$ cells in *Rasa3*$^{flox/flox}$*Cd4Cre* mice (Figure 2f), although Foxp3$^+$ Treg cell population remained unaffected (Figure S2b). Consistently, spinal cord-infiltrating RASA3-deficient CD4$^+$ T cells expressed decreased levels of pTh17-related genes including *Rorc, Il17a, Il23r* and *Csf2,* but increased level of non-pathogenic-Th17-related gene *Il10* (Figure 2g). These findings indicate that RASA3 is required for the generation of pTh17 cells to cause tissue immune-pathology and subsequent autoimmunity.

## Loss of RASA3 leads to a dominant trans-repression of pTh17 cell generation via soluble factors of Th2-bias.

To reveal the mechanisms underlying the critical role for RASA3 in pTh17 generation, we firstly addressed if RASA3 deletion led to a dominant or recessive effect to limit pTh17 generation by mixing RASA3-deficient and -sufficient T cells during pTh17 cell differentiation. We found that, while RASA3-deficient cells remained defective in producing IL-17A, co-exiting wild-type cells also became unable to produce IL-17A (Figure 3a), suggesting that RASA3 deletion led to a dominant, trans-repression of pTh17 cell generation. Such an effect was likely due to soluble factor(s) produced by RASA3-deficient cells, as RASA3-deficient pTh17 cell conditioned medium inhibited pTh17 differentiation of wild-type cells (Figure 3b) and their expression of pTh17-cell-related genes (Figure 3c).

We therefore sought to identify how the expression of genes, especially the cytokines, were altered in RASA3-deficient cells during pTh17 differentiation by using genome-wide RNA-seq analysis. Compared to RASA3-sufficient T cells, RASA3-deficient T cells expressed less Th17 cell related genes, including *Il17a* and *Rorc*, during pTh17 cell differentiation (Figure S3a). However, we found that Th2, but not Th1, cytokines and related genes were aberrantly upregulated in RASA3-deficient cells as early as 6 hours post activation under pTh17 cell polarizing condition (Figure 3d, 3e and 3f and Figure S3b). Consistently, the percentages of IL-4$^+$ and IL-10$^+$ cells increased in the absence of RASA3 during pTh17 differentiation *in vitro* (Figure 3g). Furthermore, spinal-cord-infiltrating RASA3-deficient CD4$^+$ T cells expressed increased levels of Th2-realated genes during EAE (Figure S3c). The aforementioned findings therefore suggest that RASA3 is required to restrict Th2-related program in developing pTh17 cells.

### Defective pTh17 cell generation in the absence of RASA3 is due to aberrant IL-4 expression.

The findings from the genome-wide RNA-seq analysis suggested that aberrantly upregulated IL-4 and/or IL-10 may account for defective pTh17 cell generation in the absence of RASA3. By using antibodies against IL-4 and IL-10, we found that neutralizing IL-4 (Figure 4a), but not IL-10 (Figure S4a), restored the capacity of RASA3-deficient $CD4^+$ T cell to differentiate into pTh17 cells *in vitro*. In addition, neutralizing IL-4 (Figure 4b) but not IL-10 (Figure S4b) abolished the ability of RASA3-deficient $CD4^+$ T cells to dominantly trans-repress pTh17 cell generation of wild-type $CD4^+$ T cells *in vitro*. Elevated IL-10 production by RASA3-deficient $CD4^+$ T cells depended on IL-4, because IL-4 neutralization hampered IL-10 upregulation in these cells (Figure 4c). Deletion of IL-4 in RASA3-deficient cells not only restored pTh17 cell 9 generation and the expression of pTh17-cell-related genes but also reduced IL-10 production and the Th2-bias program of RASA3-deficient $CD4^+$ T cells *in vitro* (Figure 4d and 4e).

IL-4 was critical to inhibit pTh17 cell generation in the absence of RASA3 during EAE development *in vvivo*. $IL\text{-}4^+$ cells were increased in the spinal-cords of *Rasa3*$^{flox/flox}$*Cd4Cre* mice during EAE development (Figure S4c) suggesting a role for IL-4 to reduce EAE disease in these mice (Figure 2). Antibody-mediated neutralization of IL-4 largely restored EAE development in *Rasa3*$^{flox/flox}$*Cd4Cre* mice (Figure S4d, S4e, S4f) and pTh17 cell generation (Figure S4g), and normalized IL-10 production in the spinal-cord (Figure S4h). Deletion of IL-4 restored EAE development of *Rasa3*$^{flox/flox}$*Cd4Cre* mice (Figure 4f and 4g). The defective pTh17 cell generation, aberrant IL-10 production and Th2 bias observed in the spinal-cord-infiltrating T cells in *Rasa3*$^{flox/flox}$*Cd4Cre* mice were corrected when IL-4 was deleted (Figure 4h, 4i and Figure S4i). These findings suggest that RASA3 is critical to control the reciprocal pTh17 and Th2 programs. Lack of RASA3 causes $CD4^+$ T cell to deviate from pTh17 cell and bias towards Th2 function, which in turn restricts pTh17 cell generation in an IL-4 dependent manner.

### RASA3 controls IL-4 expression during pTh17 cell generation via interferon regulatory factor 4 (IRF4).

Aforementioned findings promoted us to determine the molecular mechanisms through which RASA3 regulates IL-4 expression. GATA3, IRF4, c-Maf and STAT6-phosphrylation are central to Th2 program (Ho et al., 1998; Lohoff et al., 2002; Rengarajan et al., 2002; Zheng and Flavell, 1997) and are found upregulated in RASA3- deficient $CD4^+$ T cells during pTh17 cell generation (Figure 5a and Figure S5a). Nonetheless, because IL-4 promotes Th2 programs through feed-forward mechanisms, it is possible that some of the observed upregulation was a “result” rather than the “cause” of the aberrant IL-4 upregulation in the RASA3-deficient pTh17 cells. To distinguish the two possibilities, we abrogated IL-4 by either using neutralizing antibody or genetic deletion. The upregulation of IRF4, but not that of GATA3, c-Maf and STAT6- phosphorylation, in RASA3-deficient $CD4^+$ T cells was independent of IL-4 (Figure 5b, 5c and Figure S5b), suggesting that IRF4 upregulation caused IL-4 increase in RASA3-deficient cells. Indeed, short hairpin RNA (shRNA)-mediated IRF4 knockdown in RASA3-deficient cells (Figure 5d) normalized IL-4 expression and Th2-related program (Figure 5e), and restored pTh17 cell generation (Figure

5f) and pTh17-cell-related programs (Figure 5g). In addition, we found that RASA3 and IRF4 expression were reciprocally regulated during pTh17 and Th2 cell generation (Figure S5c), and that ectopically expressed IRF4 suppressed pTh17-related program but promoted Th2-related program during pTh17 cell generation specifically (Figure S5d). Aforementioned findings suggest that RASA3-IRF4 axis balances pTh17- and Th2-related program to specifically direct pTh17 cell generation.

### RASA3 bridges the interaction between Cbl proto-oncogene-b (Cbl-b) and IRF4 for IRF4 degradation.

Because we found that RASA3 balanced pTh17-Th2 programs via IRF4, we further investigated how RASA3 regulates IRF4 expression. In the absence of RASA3, IRF4 mRNA expression did not increase during pTh17 cell generation (Figure S6a), suggesting that IRF4 upregulation occurred via a post-transcriptional mechanism. Indeed, IRF4 protein stability greatly enhanced in RASA3-deficient pTh17 cells (Figure 6a). Proteasome-dependent protein degradation was found important to control IRF4 protein stability, as the inhibition of proteasome activity increased IRF4 expression in the wild-type cells to a similar level as in RASA3-deficient cells (Figure 6b).

RASA3 controls IRF4 protein stability likely through a direct mechanism, because by combining immunoprecipitation and unbiased mass-spectrometry (IP-MS) analysis, we found that RASA3 bound to IRF4, but not GATA3 or c-Maf, during pTh17 cell differentiation (Figure S6b and S6c). The IP-MS approach also revealed that RASA3 interacted with E3-ubiquitin ligases, among which Cbl proto-oncogene-b (Cbl-b) is known to suppress Th2 differentiation (Qiao et al., 2014) (Figure S6b and S6d). RASA3 indeed interacted with IRF4 and Cbl-b during pTh17 cell generation, detected by endogenous co-immunoprecipitation assays (Figure 6c and Figure S6e). In addition, we found that IRF4 and Cbl-b interact with each other and such an interaction requires RASA3 because the interaction between IRF4 and Cbl-b became much weaker upon RASA3 deletion (Figure 6d).

These findings suggest that RASA3 facilitates Cbl-b to interact with IRF4 to degrade IRF4 via poly-ubiquitination. In 293T cells where RASA3 is barely expressed, ectopically expressed IRF4 and Cbl-b did not interact strongly until RASA3 was introduced (Figure S6f). RASA3 expression promoted IRF4 protein poly-ubiquitination (Figure 6e) and proteasome-mediated degradation in a Cbl-b dependent manner (Figure 6e and Figure S6g). Therefore, RASA3 is required for Cbl-b to interact with IRF4 to mediate the poly-ubiquitination and degradation of IRF4. These results indicate that RASA3 bridges the interaction of Cbl-b to IRF4 to promote IRF4 protein degradation.

Collectively, aforementioned findings reveal an essential role for RASA3 in directing pTh17 cell generation by counter-balancing Th2-related program through restraining IRF4 function. RASA3 does so mechanistically by mediating the interactions between E3 ubiquitin Ligase Cbl-b and IRF4 to promote IRF4 protein degradation (Figure S6h).

## DISCUSSION

Since the first description of IL-17-producing Th17 cells, such cell type attracts great attention for its vital role in promoting immune response and causing immune pathology in myriad immune-related diseases (Dong, 2008; Korn et al., 2009; Patel and Kuchroo, 2015; Zou and Restifo, 2010). Subsequent studies however reveal that IL-17-producing cells may also possess immune regulatory function (Esplugues et al., 2011; McGeachy et al., 2007; Stumhofer et al., 2007), suggesting that Th17 cells' function is more diverse and context-dependent than previously thought. Indeed, different cytokine combinations endow Th17 cells with pathogenic (IL-1β+IL-6+IL-23) or non-pathogenic (TGF-β+IL-6) functions. In addition, the molecular programs of pathogenic and non-pathogenic-Th17 cell are quite different (Gaffen et al., 2014; Lee et al., 2012). These findings beg the question if pathogenic and non-pathogenic-Th17 cells can be classified as distinct Th17 cell subtypes or mere functional adaptations of Th17 cells to the environmental cues. Previous available evidence supports the latter, because critical factors including IL-23-IL-23R and CD5L contribute to the pathogenicity, but not the generation, of Th17 cells (Langrish et al., 2005; Stritesky et al., 2008; Wang et al., 2015). The current study offered the evidence to support the notion that unique molecular programs including RASA3 indeed exist to diverge pathogenic-Th17 cell generation from non-pathogenic-Th17 cell generation. It is therefore likely that, to achieve the functional diversification of Th17 cells, both lineage development and functional adaptation are involved.

Despite Th cell subsets are functionally distinct and engage cell-type specific molecular networks, they do share common molecular modules to permit mutual regulation, may it be antagonism or synergism. In particular, TGF-β1+IL-6 polarized non-pathogenic-Th17 cells share genetic and epigenetic features with Th1, Th2 and Treg cells (O'Shea and Paul, 2010; Zhou et al., 2009). It is thought to be the molecular underpinning of functional malleability of Th17 cells towards Th1, Th2 and Treg cells (Bending et al., 2009; Gagliani et al., 2015; Harbour et al., 2015; Panzer et al., 2012; Zhou et al., 2009). Because pathogenic and non-pathogenic-Th17 cells have been distinguished only in recent years, whether pathogenic-Th17 cells, like non-pathogenic-Th17 cells, possess such a diverse malleability with broadly shared molecular modules of other Th cell subsets is a question of interest. Available evidence suggests that pathogenic-Th17 cells adopt Th1 signatures rather readily. In fact, T-bet, a Th1 master regulator has been associated with pathogenic-Th17 cells (Yang et al., 2009), suggesting that pathogenic-Th17 and Th1 cell generation are compatible. Conversely, pathogenic-Th17 and Th2 generation appears reciprocal (Choy et al., 2015; Harrington et al., 2005). Our finding that RASA3 is required for pathogenic-Th17 cell generation by restraining Th2 program highlights an antagonism between pathogenic-Th17 and Th2 programs and thus provides much needed mechanistic insights for above-mentioned observations. It is therefore plausible that, compared to non-pathogenic-Th17 cells, the functional malleability of pathogenic-Th17 cells is more limited. A question warrants further investigation.

The mutual regulation between pathogenic-Th17 and Th2-related programs does not occur by chance, because IRF4, a classical Th2 promoting factor (Lohoff et al., 2002; Rengarajan et al., 2002), is also essential for Th17 cell generation (Brustle et al., 2007; Ciofani et al., 2012). These observations seemingly contradict our observation that RASA3 controls the reciprocal programs of pathogenic-Th17 and Th2 cells through IRF4. Nonetheless, our findings suggest that the levels of IRF4 expression appeared to be critical: high levels of IRF4 expression suppressed and medium levels of IRF4 expression enhanced the pathogenic-Th17 cell generation of RASA3-deficent $CD4^{+}$ T cells. Yet, low levels of IRF4 expression led to a reduction of pathogenic-Th17 cell generation of these cells. These findings suggest that IRF4 controls pathogenic-Th17 program in a dose-dependent manner. Medium levels of IRF4 expression is required to promote pathogenic-Th17 program and yet high levels of IRF4 expression conversely restrict pathogic-Th17 programs by favoring Th2 program. Therefore, IRF4 serves as a sensitive and critical “rheostat” to control pathogenic-Th17 cell generati on and the reciprocal programs of pathogenic-Th17 and Th2 cells. These findings echoes accumulating evidence to suggest that an important way for IRF4 to control diverse functions in various immune cell subsets is through its expression levels (Krishnamoorthy et al., 2017; Li et al., 2018; Man et al., 2013; Ochiai et al., 2013; Yao et al., 2013). The mechanisms underlying such a dose-dependent IRF4 function has been attributed to its ability to be recruited toward target sites to control gene expression and gene locus accessibility in order to program different cell fates and functions. The greater IRF4 abundance permits its binding to low-affinity binding sites in the genome. A large numbers of promoters and enhancers involved in gene regulation are regulated by IRF4 in a dose-dependent manner in a cell type specific fashion (Krishnamoorthy et al., 2017; Man et al., 2013; Ochiai et al., 2013; Yao et al., 2013). It is therefore predicted that different levels of IRF4 expression observed in pathogenic-, non-pathogenic-Th17 and Th2 cells lead to discrete IRF4 binding patterns in the genome. What genetic loci are differentially bound by IRF4 in a16 dose-dependent manner and how they contribute to pathogenic-, non-pathogenic-Th17 and Th2 cell generation are questions warranted future investigation. In addition, in order to target pathogenic-Th17 cell function to treat related immune diseases, identifying factors besides RASA3 in fine-tuning IRF4 expression would be of interest.

IRF4 plays multi-faceted roles in controlling diverse T cell functions including Th2 and Th17 cell generation (Huber and Lohoff, 2014). We now discovered that IRF4 balances the pathogenic-Th17 and Th2 programs in a RASA3 dependent manner for pathogenic-Th17 cell generation, and that RASA3 does so through a previously unappreciated mechanism by protein degradation. Proteomic approaches revealed that RASA3 and IRF4 belong to protein complex containing E3-ubiquitin ligases including Cbl-b. The current study focused on elucidating the role for Cbl-b, due to its known role in controlling Th2 differentiation, in mediating RASA3-dependent IRF4 poly-ubiquitination and degradation. Nonetheless, several other E3-ubiquitin ligases, including Cbl, Prpf19 and Trim21, also belong to RASA3-IRF4 interactome and may contribute to IRF4 regulation. In addition, because above mentioned E3-ubiquitin ligases may have diverse targets, it warrants further investigation whether and how factors other than IRF4 contribute to RASA-directed pathogenic Th17 cell differentiation. Current findings support the notion that protein degradation is critical to control Th17 cell function, which is agreed by increasing evidences (Kathania et al., 2016; Rutz et al., 2015; Zhang et al., 2017). Such a notion remains an important and yet poorly addressed proposition that warrants further investigation to reveal “druggable “ ubiquitin ligases for treating Th17-related pathology and diseases.

# STAR★METHODS

## KEY RESOURCES TABLE

## CONTACT FOR REAGENT AND RESOURCE SHARING

Further information and requests for resources and reagents should be directed to and will be fulfilled by Yisong Wan (wany@email.unc.edu).

## EXPERIMENTAL MODEL AND SUBJECT DETAILS

**Mice—***Cd4Cre*, *Rasa3*$^{\text{flox/flox}}$ (Stefanini et al., 2015), *Il4*$^{-/-}$ , CD45.1 congenic and wild-type mice were on the C57BL/6 background. Mice used for experiments were 8–12-week old and sex (both males and females) and age matched. Littermates were used unless stated otherwise. All mice were housed and bred in specific pathogen-free conditions in the animal facility at the University of North Carolina at Chapel Hill. All mouse experiments were approved by the Institution Animal Care and Use Committee of the University of North Carolina. We complied with all relevant ethical regulations.

## METHOD DETAILS

**Flow-cytometry—**Lymphocytes were isolated from various organs of age- and sex-matched, 6–18 week old mice. Fluorescence-conjugated anti-CD25 (PC61.5), anti-CD44 (IM7), anti-CD62L (MEL-14), anti-Foxp3 (FJK16S), anti-IL-10 (JES5) (eBioscience), and anti-CD45.2 (104), anti-CD4 (RM4–5), anti-CD8 (53–6.7), anti-IFN-γ (XMG1.2), anti-IL17A (TC11–18H10.1), anti-IL-4 (11B11) (Biolegend), and Annexin V/7-amino-actinomycin D (BD Biosciences) were used. For intracellular cytokine staining, lymphocytes were stimulated for 4 hours with 50 ng/ml of PMA (phorbol 12-myristate 13-acetate) and 1μM ionomycin in the presence of brefeldin A. Staine d cells were analyzed on LSRFortessa station (BD Biosciences) or Canto (BD Biosciences).

**T cell activation, differentiation and proliferation in vitro—**CD4$^+$ T cells were isolated by mouse CD4 magnetic beads (Miltenyi Biotec) per manufacture's protocols. Isolated T cells were activated by plates coated with 10μg/ml anti-CD3 (145–2C11, BioXCell) and 10μg/ml anti-CD28 (37.51, BioXCell) and cultured in serum-free X-VIVO 20 medium (Lonza). For pathogenic-Th17 cell differentiation, 20ng/ml IL-1β (Biolegend), 20ng/ml IL-6 (Biolegend), 50ng/ml IL-23 (Biolegend) and 20μg/ml anti-IFN- γ (XMG1.2, BioXcell) were added to the culture. For non-pathogenic Th17 cell differentiation, 1ng/ml TGF-β (Biolegend), 40ng/ml IL-6 (Biolegend) and 20μg/ml anti-IFN- γ (XMG1.2, BioXcell) were added to the culture. For Th1 cell differentiation, 20ng/ml IL-12 (Biolegend) and 20ug/ml anti-IL-4 (11B11, BioXcell) were added to the culture. For Th2 cell differentiation, 40ng/ml IL-4 (Biolegend) and 20μg/ml anti-IFN- γ (XMG1.2, BioXcell) were added to the culture. Varying amounts of neutralizing anti-IL-10 (JES5–2A5, BioXcell) and anti-IL-4 (11B11, BioXcell) were added when needed as indicated. To assess proliferation, isolated CD4$^+$ T Cells were labeled with 5μM carboxyfluorescein diacetate succinimidyl ester (CFSE, BD Bioscience) for 5 minutes at the room temperature. Labelled T cells were activated under various Th17 differentiation conditions as indicated. The T cell proliferation was assessed 72 hours post activation based on CFSE dilution by flow-cytometry.

**Elicitation and analysis of experimental autoimmune encephalomyelitis (EAE) in mice—**50μg murine myelin oligodendrocyte glycoprotein (MOG) peptide 35–55 (AnaSpec) was emulsified in complete Freund's adjuvant (CFA) that consists incomplete Freund's adjuvant (Difco Laboratories) and 5mg/ml of *Mycobacterium tuberculosis* H37RA (Difco Laboratories). MOG/CFA was injected sub-cutaneous (s.c.) on day 0. 200ng Pertussis toxin (List Biological) was injected intra-peritoneal (i.p.) on day 0 and day 2. The severity of EAE was monitored and graded on a clinical score of 0 to 5: 0 = no clinical signs; 1 = Limp tail; 2 = Para-paresis (weakness, incomplete paralysis of one or two hind limbs); 3 = Paraplegia (complete paralysis of two hind limbs); 4 = Paraplegia with forelimb weakness or paralysis; 5 = Moribund or death.

After EAE elicitation, diseased mice were sacrificed and perfused with ice-cold phosphate buffered saline containing 20U/ml heparin. Spinal cord was separated from spine columns after removal of all tissues. The isolated spinal cords were subjected to pathological analysis using luxol fast blue staining. Lesions were indicated by the arrows in the figures. In addition, isolated spinal cords were digested with 1mg/ml collagenase D (Sigma) for 45 minutes at 37oC. The digested tissue was centrifuged in 38% percoll (Sigma) at 2,000 rpm for 20 minutes to separate lymphocytes. Lymphocytes were then isolated and subjected to subsequent analysis.

**Quantitative RT-PCR (qRT-PCR) and RNA-seq analysis—**For qRT-PCR analysis, total RNA was extracted from lymphocytes using TRizol reagent (Invitrogen) and reverse-transcribed into cDNA with Superscript III reverse transcriptase (Bio-Rad) per manufacturer's protocols. Quantitative PCR (qPCR) was performed on QuantStudio® 6 Flex Real-Time PCR Syst em (ThermoFisher Scientific).

For RNA-seq analysis, total RNA was extracted from T cells by using RNA-easy mini kit (Qiagen). RNA-seq libraries were generated and poly(A) enriched with 1 microgram of RNA as input using the TruSeq RNA Sample Prep Kit (Illumina, San Diego, CA). Indexed samples were sequenced using the 50bp paired-end protocol via the HiSeq 2500 (Illumina) per the manufacturer's protocol. Reads (32–45 Million reads per sample) were analyzed with Salmon [version 0.9.1] (Patro et al., 2017) software, with mm10 as reference genome, to align and quantify the transcript expression. R packages in Bioconductor, tximport and tximportData (Soneson et al., 2015) were used to aggregate transcript-level quantifications to the gene level, with the R package biomaRt for gene and transcripts mapping. The option "lengthScaledTPM" for countsFromAbundance in tximport was used to obtain the estimated counts at the gene level using abundance estimates scaled based on the average transcript length over samples and the library size. R function voom (Law et al., 2014) in limma package was used to transform the estimated count data into log2 scale and estimate the mean-variance relationship so that it can be used to compute appropriate observation level weights, followed by linear modelling. For gene-level differential expression analysis, a linear model was fitted to the log scaled expression data with the genotypes (knockout and wild-type) as one covariate using empirical Bayes moderated t-statistics (Ritchie et al., 2015). The false discovery rate (FDR) was controlled using the Benjamini and Hochberg algorithm. Probes with FDR < 0.05 and fold-change > 2 were judged to be differentially expressed. 317 and 35 genes were identified to be significantly up- and down-regulated respectively. Barcode plots were generated to show the differential expression patterns and to calculate the enrichment scores of Th1/Th2 (KEGG mmu04658) and Th17 (KEGG mmu04659) related genes in the knockout vs. wild-type comparisons. The R function CAMERA (Wu and Smyth, 2012) was used to determine whether each gene set was differentially expressed in the comparisons as a set. R version 3.4.3 was used.

**Immuno-blotting, Immuno-precipitation (IP) and Mass-Spectrometry (MS)—**For immune-blotting, protein extracts were resolved by Any kD™ Mini-PROTEAN® TGX™ Precast Protein Gels (Bio-Rad), trans ferred to a polyvinylidene fluoride membrane (Millipore) and analyzed by immuno-blotting with the following antibodies: anti-RASA3 (rabbit anti-RASA3 serum generated by Dr. Wolfgang Bergmeier, UNC-CH), anti-GATA3 (L50–823; BD), anti-HA-HRP (3F10; Sigma), anti-β-actin (I-19; Santa Cruz), anti-IRF4 (D9P5H, CST), anti-phospho-STAT3 Y705 (D3A7, CST), anti-STAT3 (79D7, CST), anti-phospho-STAT6 Thy641 (CST), anti-STAT6 (CST), anti-BATF (WW8, Santa Cruz), anti-c-Maf (55013-AP, Proteintech Group), anti-Flag (M2, Sigma) and anti-Cbl-b (G-1, Santa Cruz).

For IP, cells were lysed with IP lysis buffer (10 mM HEPES, pH 7.5, 1.5mM $MgCl_2$, 0.2 mM EDTA and 150mM NaCl containing 1% NP40) and sonicated with Bioruptor PICO. Cell lysates were incubated with 50μl magnetic protein A/G beads (Bio-rad) conjugated with antibodies treated by dimethyl pimelimidate or anti-Flag M2 magnetic beads (Sigma). After overnight incubation, beads were washed 4 times with lysis buffer. Associated protein was eluted by Laemmli sample buffer (Bio-Rad) and incubated at 95 °C for 5 min. Eluted samples were s eparated by SDS-PAGE gel and analyzed by immuno-blotting.

For MS analysis, immuno-precipitated proteins were eluted with buffer containing 8M Urea, 50mM Tris (pH 8.0), reduced with 5mM DTT and alkylated with 15mM iodoacetamide. Trypsin digestion was performed at room temperature overnight in final 2M urea buffer. The peptides were desalted on C18 stage-tips and dissolved in 0.1% formic acid. Peptides were loaded on an EASY-Spray C18 Column (Thermo Fisher Scientific) and analyzed on a Q-Exactive HF coupled with an Easy nanoLC 1200 (Thermo Fisher Scientific). Analytical separation of all the tryptic peptides was achieved with a linear gradient of 2–40% buffer B over 45 mi n followed a ramp to 100% B in 3-min and 12-min wash with 100% buffer B, where buffer A was aqueous 0.1% formic acid, and buffer B was solution containing 80% acetonitrile and 0.1% formic acid. LC-MS experiments were performed in a data-dependent mode with full MS (externally calibrated to a mass accuracy of <5 ppm and a resolution of 60,000 at *m/z* 200) followed by high energy collision-activated dissociation-MS/MS of the top 20 most intense ions with a resolution of 15,000 at *m/z* 200. High energy collision-activated dissociation-MS/MS was used to dissociate peptides at a normalized collision energy (NCE) of 26 eV. Dynamic exclusion with 20.0 seconds was enabled. Then the mass spectra were processed, and peptide identification was performed using the Andromeda search engine found in MaxQuant software version 1.6.0.16 (Max Planck Institute, Germany) against the UniProt mouse protein sequence database (UP000000589). Peptides were identified with a target-decoy approach using a combined database consisting of reverse protein sequences of the database. Up to two missed cleavages was allowed. Peptide identifications are reported by filtering of reverse and contaminant entries and assigning to their leading razor protein. Peptide inference and proteins identification were filtered to maximum 1% and 5% false discovery rate (FDR), respectively. Data processing and statistical analysis were performed on Perseus (Version 1.6.0.7). A two samples t-test statistics was used with a p-value < 0.05 to report statistically significant expression.

**Ectopic gene expression and shRNA-mediated gene knock down—**For ectopic gene expression, full-length cDNA encoding IRF4, RASA3 and Cbl-b (Transomics) were cloned into pCMV-Flag vector, MSCV-IRES-EGFP (MIG) vector or MSCV-IRES-Thy1.1 (MIT) vectors. For shRNA-mediated gene knockdown, lenti-viral shRNA constructs carrying puromycin resistance genes (MISSION shRNA library, Sigma) were purchased from shRNA core facility of UNC Chapel Hill. Scrambled shRNA constructs (pLKO.1-scramble shRNA control) carrying puromycin resistance gene was obtained from Addgene.

Lentiviruses and retroviruses were prepared by transfecting HEK293T cells. Activated T cells were spin inoculated with recombinant viruses by centrifuging at 1,500 x g for 2 hours at 30$^{o}$C with 10mM HEPES and 8μg/ml polybrene. Antibiotic selection was performed, when applicable, by adding 2μg/ml puromycin in the culture medium. The transduced cells were then identified based on puromycin resistance or Thy1.1 positive.

**Lamina propria leukocytes isolation—**Small or large intestine was mechanically dissected and flushed with ice-cold PBS. The intestines were cut into 8 pieces and incubated in the presence of 1mM DTT and 5mM EDTA at 37$^{o}$C for 30 min. The digested pieces were passed through a 100μm cell strainer. The cell suspension was discarded. The remaining pieces were cut into 1mm pieces and further digested in RPMI 1640 medium with collagenase D (1mg/ml collagenase D, Roche), DNase I (100μg/ ml, Sigma), Liberase TL (0.2mg/ml, Roche) and 10% FBS at 37°C for 1h. The LPL were isolated by ce ntrifuging at 2000rpm for 20 min with 40% and 80% discontinuous Percoll density gradient (Sigma). Isolated LPL were then subjected to subsequent analysis.

**Statistical analysis—**Two-tailed/sided Student's *t*-test was used to compare two groups of samples. Mann-Whitney test was used to compare multiple groups of samples in EAE experiments. p<0.05 (confidence interval of 95%) was considered statistically significant. In the figures, *, ** and *** were used to indicate p<0.05, p<0.01 and p<0.001 respectively. All results shown are mean ± s.d. unless stated otherwise.

### DATA AND SOFTWARE AVAILABILITY

RNA-seq data are deposited in GEO database under ID code: GSE111473.

## Supplementary Material

Refer to Web version on PubMed Central for supplementary material.

## ACKNOWLEGEMENT:

We thank N. Fisher (University of North Carolina Flow-cytometry facility support in part by P30 CA016086 Cancer Center Core Support Grant), supports from the National Natural Science Foundation of China (81402549, LJQ2015033) for G.Z., from NIH/NHLBI (HL130404) for W.B, and from NIH/NIAID (AI097392; AI123193), National Multiple Sclerosis Society (NMSS), and Yang Family Biomedical Scholars Award for Y.Y.W.

## REFERENCES

### References

Ahern PP, Schiering C, Buonocore S, McGeachy MJ, Cua DJ, Maloy KJ, and Powrie F (2010). Interleukin-23 drives intestinal inflammation through direct activity on T cells. Immunity 33, 279–288. [PubMed: 20732640]

Bending D, De la Pena H, Veldhoen M, Phillips JM, Uyttenhove C, Stockinger B, and Cooke A (2009). Highly purified Th17 cells from BDC2.5NOD mice convert into Th1-like cells in NOD/SCID recipient mice. The Journal of clinical investigation 119, 565–572. [PubMed: 19188681]

Bettelli E, Carrier Y, Gao W, Korn T, Strom TB, Oukka M, Weiner HL, and Kuchroo VK (2006). Reciprocal developmental pathways for the generation of pathogenic effector TH17 and regulatory T cells. Nature 441, 235–238. [PubMed: 16648838]

Bettelli E, Korn T, Oukka M, and Kuchroo VK (2008). Induction and effector functions of T(H)17 cells. Nature 453, 1051–1057. [PubMed: 18563156]

Brustle A, Heink S, Huber M, Rosenplanter C, Stadelmann C, Yu P, Arpaia E, Mak TW, Kamradt T, and Lohoff M (2007). The development of inflammatory T(H)-17 cells requires interferon-regulatory factor 4. Nature immunology 8, 958–966. [PubMed: 17676043]

Choy DF, Hart KM, Borthwick LA, Shikotra A, Nagarkar DR, Siddiqui S, Jia G, Ohri CM, Doran E, Vannella KM, et al. (2015). TH2 and TH17 inflammatory pathways are reciprocally regulated in asthma. Science translational medicine 7, 301ra129.

Chung Y, Chang SH, Martinez GJ, Yang XO, Nurieva R, Kang HS, Ma L, Watowich SS, Jetten AM, Tian Q, et al. (2009). Critical regulation of early Th17 cell differentiation by interleukin-1 signaling. Immunity 30, 576–587. [PubMed: 19362022]

Ciofani M, Madar A, Galan C, Sellars M, Mace K, Pauli F, Agarwal A, Huang W, Parkhurst CN, Muratet M, et al. (2012). A validated regulatory network for Th17 cell specification. Cell 151, 289–303. [PubMed: 23021777]

Dong C (2008). TH17 cells in development: an updated view of their molecular identity and genetic programming. Nature reviews Immunology 8, 337–348.

El-Behi M, Ciric B, Dai H, Yan Y, Cullimore M, Safavi F, Zhang GX, Dittel BN, and Rostami A (2011). The encephalitogenicity of T(H)17 cells is dependent on IL-1- and IL-23-induced production of the cytokine GM-CSF. Nature immunology 12, 568–575. [PubMed: 21516111]

Esplugues E, Huber S, Gagliani N, Hauser AE, Town T, Wan YY, O'Connor W, Jr., Rongvaux A, Van Rooijen N, Haberman AM, et al. (2011). Control of TH17 cells occurs in the small intestine. Nature 475, 514–518. [PubMed: 21765430]

Fontenot JD, Gavin MA, and Rudensky AY (2003). Foxp3 programs the development and function of CD4+CD25+ regulatory T cells. Nat Immunol 4, 330–336. [PubMed: 12612578]

Gaffen SL, Jain R, Garg AV, and Cua DJ (2014). The IL-23-IL-17 immune axis: from mechanisms to therapeutic testing. Nature reviews Immunology 14, 585–600.

Gagliani N, Amezcua Vesely MC, Iseppon A, Brockmann L, Xu H, Palm NW, de Zoete MR, Licona-Limon P, Paiva RS, Ching T, et al. (2015). Th17 cells transdifferentiate into regulatory T cells during resolution of inflammation. Nature 523, 221–225. [PubMed: 25924064]

Ghoreschi K, Laurence A, Yang XP, Tato CM, McGeachy MJ, Konkel JE, Ramos HL, Wei L, Davidson TS, Bouladoux N, et al. (2010). Generation of pathogenic T(H)17 cells in the absence of TGF-beta signalling. Nature 467, 967–971. [PubMed: 20962846]

Harbour SN, Maynard CL, Zindl CL, Schoeb TR, and Weaver CT (2015). Th17 cells give rise to Th1 cells that are required for the pathogenesis of colitis. Proc Natl Acad Sci U S A 112, 7061–7066. [PubMed: 26038559]

Harrington LE, Hatton RD, Mangan PR, Turner H, Murphy TL, Murphy KM, and Weaver CT (2005). Interleukin 17-producing CD4+ effector T cells develop via a lineage distinct from the T helper type 1 and 2 lineages. Nat Immunol 6, 1123–1132. [PubMed: 16200070]

Ho IC, Lo D, and Glimcher LH (1998). c-maf promotes T helper cell type 2 (Th2) and attenuates Th1 differentiation by both interleukin 4-dependent and -independent mechanisms. J Exp Med 188, 1859–1866. [PubMed: 9815263]

Hori S, Nomura T, and Sakaguchi S (2003). Control of regulatory T cell development by the transcription factor Foxp3. Science 299, 1057–1061. [PubMed: 12522256]

Huber M, and Lohoff M (2014). IRF4 at the crossroads of effector T-cell fate decision. European journal of immunology 44, 1886–1895. [PubMed: 24782159]

Ivanov II, McKenzie BS, Zhou L, Tadokoro CE, Lepelley A, Lafaille JJ, Cua DJ, and Littman DR (2006). The orphan nuclear receptor RORgammat directs the differentiation program of proinflammatory IL-17+ T helper cells. Cell 126, 1121–1133. [PubMed: 16990136]

Kathania M, Khare P, Zeng M, Cantarel B, Zhang H, Ueno H, and Venuprasad K (2016). Itch inhibits IL-17-mediated colon inflammation and tumorigenesis by ROR-gammat ubiquitination. Nature immunology 17, 997–1004. [PubMed: 27322655]

Korn T, Bettelli E, Oukka M, and Kuchroo VK (2009). IL-17 and Th17 Cells. Annu Rev Immunol 27, 485–517. [PubMed: 19132915]

Langrish CL, Chen Y, Blumenschein WM, Mattson J, Basham B, Sedgwick JD, McClanahan T, Kastelein RA, and Cua DJ (2005). IL-23 drives a pathogenic T cell population that induces autoimmune inflammation. J Exp Med 201, 233–240. [PubMed: 15657292]

Law CW, Chen Y, Shi W, and Smyth GK (2014). voom: Precision weights unlock linear model analysis tools for RNA-seq read counts. Genome Biol 15, R29. [PubMed: 24485249]

Lee Y, Awasthi A, Yosef N, Quintana FJ, Xiao S, Peters A, Wu C, Kleinewietfeld M, Kunder S, Hafler DA, et al. (2012). Induction and molecular signature of pathogenic TH17 cells. Nature immunology 13, 991–999. [PubMed: 22961052]

Lohoff M, Mittrucker HW, Prechtl S, Bischof S, Sommer F, Kock S, Ferrick DA, Duncan GS, Gessner A, and Mak TW (2002). Dysregulated T helper cell differentiation in the absence of interferon regulatory factor 4. Proc Natl Acad Sci U S A 99, 11808–11812. [PubMed: 12189207]

McGeachy MJ, Bak-Jensen KS, Chen Y, Tato CM, Blumenschein W, McClanahan T, and Cua DJ (2007). TGF-beta and IL-6 drive the production of IL-17 and IL-10 by T cells and restrain T(H)-17 cell-mediated pathology. Nature immunology 8, 1390–1397. [PubMed: 17994024]

McGeachy MJ, Chen Y, Tato CM, Laurence A, Joyce-Shaikh B, Blumenschein WM, McClanahan TK, O'Shea JJ, and Cua DJ (2009). The interleukin 23 receptor is essential for the terminal differentiation of interleukin 17-producing effector T helper cells in vivo. Nature immunology 10, 314–324. [PubMed: 19182808]

Mosmann TR, Cherwinski H, Bond MW, Giedlin MA, and Coffman RL (1986). Two types of murine helper T cell clone. I. Definition according to profiles of lymphokine activities and secreted proteins. Journal of immunology 136, 2348–2357.

O'Shea JJ, and Paul WE (2010). Mechanisms underlying lineage commitment and plasticity of helper CD4+ T cells. Science 327, 1098–1102. [PubMed: 20185720]

Panzer M, Sitte S, Wirth S, Drexler I, Sparwasser T, and Voehringer D (2012). Rapid in vivo conversion of effector T cells into Th2 cells during helminth infection. Journal of immunology 188, 615–623.

Park H, Li Z, Yang XO, Chang SH, Nurieva R, Wang YH, Wang Y, Hood L, Zhu Z, Tian Q, et al. (2005). A distinct lineage of CD4 T cells regulates tissue inflammation by producing interleukin 17. Nature immunology 6, 1133–1141. [PubMed: 16200068]

Patel DD, and Kuchroo VK (2015). Th17 Cell Pathway in Human Immunity: Lessons from Genetics and Therapeutic Interventions. Immunity 43, 1040–1051. [PubMed: 26682981]

Patro R, Duggal G, Love MI, Irizarry RA, and Kingsford C (2017). Salmon provides fast and bias-aware quantification of transcript expression. Nature methods 14, 417–419. [PubMed: 28263959]

Peters A, Lee Y, and Kuchroo VK (2011). The many faces of Th17 cells. Current opinion in immunology 23, 702–706. [PubMed: 21899997]

Qiao G, Ying H, Zhao Y, Liang Y, Guo H, Shen H, Li Z, Solway J, Tao E, Chiang YJ, et al. (2014). E3 ubiquitin ligase Cbl-b suppresses proallergic T cell development and allergic airway inflammation. Cell reports 6, 709–723. [PubMed: 24508458]

Rengarajan J, Mowen KA, McBride KD, Smith ED, Singh H, and Glimcher LH (2002). Interferon regulatory factor 4 (IRF4) interacts with NFATc2 to modulate interleukin 4 gene expression. The Journal of experimental medicine 195, 1003–1012. [PubMed: 11956291]

Ritchie ME, Phipson B, Wu D, Hu Y, Law CW, Shi W, and Smyth GK (2015). limma powers differential expression analyses for RNA-sequencing and microarray studies. Nucleic Acids Res 43, e47. [PubMed: 25605792]

Rutz S, Kayagaki N, Phung QT, Eidenschenk C, Noubade R, Wang X, Lesch J, Lu R, Newton K, Huang OW, et al. (2015). Deubiquitinase DUBA is a post-translational brake on interleukin-17 production in T cells. Nature 518, 417–421. [PubMed: 25470037]

Sakaguchi S (2000). Regulatory T cells: key controllers of immunologic self-tolerance. Cell 101, 455–458. [PubMed: 10850488]

Schraml BU, Hildner K, Ise W, Lee WL, Smith WA, Solomon B, Sahota G, Sim J, Mukasa R, Cemerski S, et al. (2009). The AP-1 transcription factor Batf controls T(H)17 differentiation. Nature 460, 405–409. [PubMed: 19578362]

Schurmans S, Polizzi S, Scoumanne A, Sayyed S, and Molina-Ortiz P (2015). The Ras/Rap GTPase activating protein RASA3: from gene structure to in vivo functions. Adv Biol Regul 57, 153–161. [PubMed: 25294679]

Soneson C, Love MI, and Robinson MD (2015). Differential analyses for RNA-seq: transcript-level estimates improve gene-level inferences. F1000Res 4, 1521. [PubMed: 26925227]

Stefanini L, Paul DS, Robledo RF, Chan ER, Getz TM, Campbell RA, Kechele DO, Casari C, Piatt R, Caron KM, et al. (2015). RASA3 is a critical inhibitor of RAP1-dependent platelet activation. J Clin Invest 125, 1419–1432. [PubMed: 25705885]

Stritesky GL, Yeh N, and Kaplan MH (2008). IL-23 promotes maintenance but not commitment to the Th17 lineage. Journal of immunology 181, 5948–5955.

Stumhofer JS, Silver JS, Laurence A, Porrett PM, Harris TH, Turka LA, Ernst M, Saris CJ, O'Shea JJ, and Hunter CA (2007). Interleukins 27 and 6 induce STAT3-mediated T cell production of interleukin 10. Nat Immunol 8, 1363–1371. [PubMed: 17994025]

Szabo SJ, Kim ST, Costa GL, Zhang X, Fathman CG, and Glimcher LH (2000). A novel transcription factor, T-bet, directs Th1 lineage commitment. Cell 100, 655–669. [PubMed: 10761931]

Wang C, Yosef N, Gaublomme J, Wu C, Lee Y, Clish CB, Kaminski J, Xiao S, Meyer Zu Horste G, Pawlak M, et al. (2015). CD5L/AIM Regulates Lipid Biosynthesis and Restrains Th17 Cell Pathogenicity. Cell 163, 1413–1427. [PubMed: 26607793]

Wu D, and Smyth GK (2012). Camera: a competitive gene set test accounting for inter-gene correlation. Nucleic Acids Res 40, e133. [PubMed: 22638577]

Yang Y, Weiner J, Liu Y, Smith AJ, Huss DJ, Winger R, Peng H, Cravens PD, Racke MK, and Lovett-Racke AE (2009). T-bet is essential for encephalitogenicity of both Th1 and Th17 cells. The Journal of experimental medicine 206, 1549–1564. [PubMed: 19546248]

Zhang S, Takaku M, Zou L, Gu AD, Chou WC, Zhang G, Wu B, Kong Q, Thomas SY, Serody JS, et al. (2017). Reversing SKI-SMAD4-mediated suppression is essential for TH17 cell differentiation. Nature 551, 105–109. [PubMed: 29072299]

Zheng W, and Flavell RA (1997). The transcription factor GATA-3 is necessary and sufficient for Th2 cytokine gene expression in CD4 T cells. Cell 89, 587–596. [PubMed: 9160750]

Zhou L, Chong MM, and Littman DR (2009). Plasticity of CD4+ T cell lineage differentiation. Immunity 30, 646–655. [PubMed: 19464987]

Zhu J, Yamane H, and Paul WE (2010). Differentiation of effector CD4 T cell populations (*). Annu Rev Immunol 28, 445–489. [PubMed: 20192806]

Zou W, and Restifo NP (2010). T(H)17 cells in tumour immunity and immunotherapy. Nature reviews Immunology 10, 248–256.

## Highlights

1. Pathogenic Th17 cell generation requires RASA3.
2. RASA3 is vital for the pathogenicity of T cells in EAE.
3. RASA3 restricts IRF4-dependent Th2 programs to favor pTh17 programs.
4. RASA3 interacts with Cbl-b to promote IRF4 protein degradation.

## In Brief

Pathogenic-Th17 cells promote immune-pathology, but how their generation is controlled remains largely unknown. Wu et.al reveal that RASA3 is essential for pathogenic Th17 cell generation but dispensable for non-pathogenic Th17 generation. RASA3 functions by repressing Th2 cell programs in pathogenic Th17 cells by fine-tuning IRF4 protein expression.

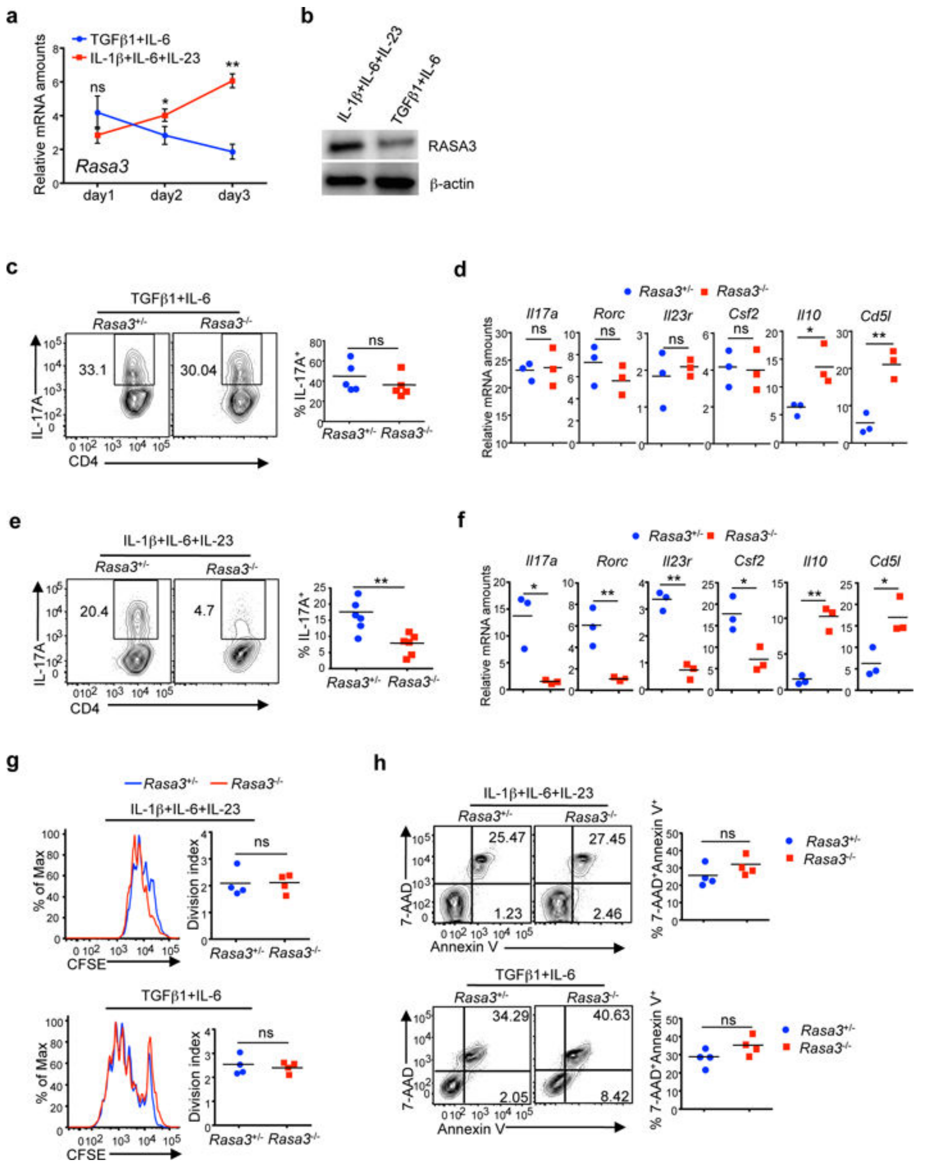


**Figure 1. RASA3 is specifically required for pathogenic-Th17 (pTh17) cell generation.**

(**a**) Comparison of RASA3 mRNA expression in CD4+ T cells activated in the presence of IL-1β+IL-6+IL-23 (pTh17 cell polarizing condition) and TGFβ1+IL-6 at indicated time points by qRT-PCR analysis. (n=3 samples from 3 independent experiments; means ± s.d., ns, not significant, *p<0.01, **p<0.01, per two-sided *t*-test)

(**b**) Immunoblotting to detect RASA3 protein expression in CD4+ T cells activated under indicated conditions for 3 days. Results are representative of 3 independent experiments.

(**c**) Flow-cytometry of IL-17A produced by CD4+ T cells of indicated genotypes, activated in the presence of TGFβ1+IL-6 for 4 days. (n=5 samples from 5 independent experiments; ns, not significant per two-sided *t*-test; centers indicate the mean values)

(**d**) qRT-PCR analysis to detect mRNA levels of Th17-related genes expressed by CD4+ T cells of indicated genotypes, activated under pTh17 cell polarizing condition for 4 days.

(n=3 samples from 3 independent experiments; ns, not significant, *p<0.01, **p<0.01, per two-sided *t*-test; centers indicate the mean values)

(**e**) Flow-cytometry of IL-17A produced by $CD4^+$ T cells of indicated genotypes, activated under pTh17 cell polarizing condition for 4 days. (n=6 samples from 6 independent experiments; **p<0.01 per two-sided *t*-test; centers indicate the mean values)

(**f**) qRT-PCR analysis to detect mRNA levels of Th17-related genes expressed by $CD4^+$ T cells of indicated genotypes, activated under pTh17 cell polarizing condition for 4 days. (n=3 samples from 3 independent experiments; *p<0.01, **p<0.01, per two-sided *t*-test; centers indicate the mean values)

(**g**) The proliferation of $CD4^+$ T cells of indicated genotypes activated in the presence of TGFβ1+IL-6 or IL-1β+IL-6+IL-23 for 3 days, assessed by CFSE dilution assay and flow-cytometry. (n=4 samples from 4 independent experiments; ns, not significant per two-sided *t*-test; centers indicate the mean values)

(**h**) The apoptosis of $CD4^+$ T cells of indicated genotypes activated in the presence of TGFβ1+IL-6 or IL-1β+IL-6+IL-23 for 2 days, monitored by Annexin V and 7-AAD staining and flow-cytometry. (n=4 samples from 4 independent experiments; ns, not significant per two-sided *t*-test; centers indicate the mean values)

See also Figure S1.

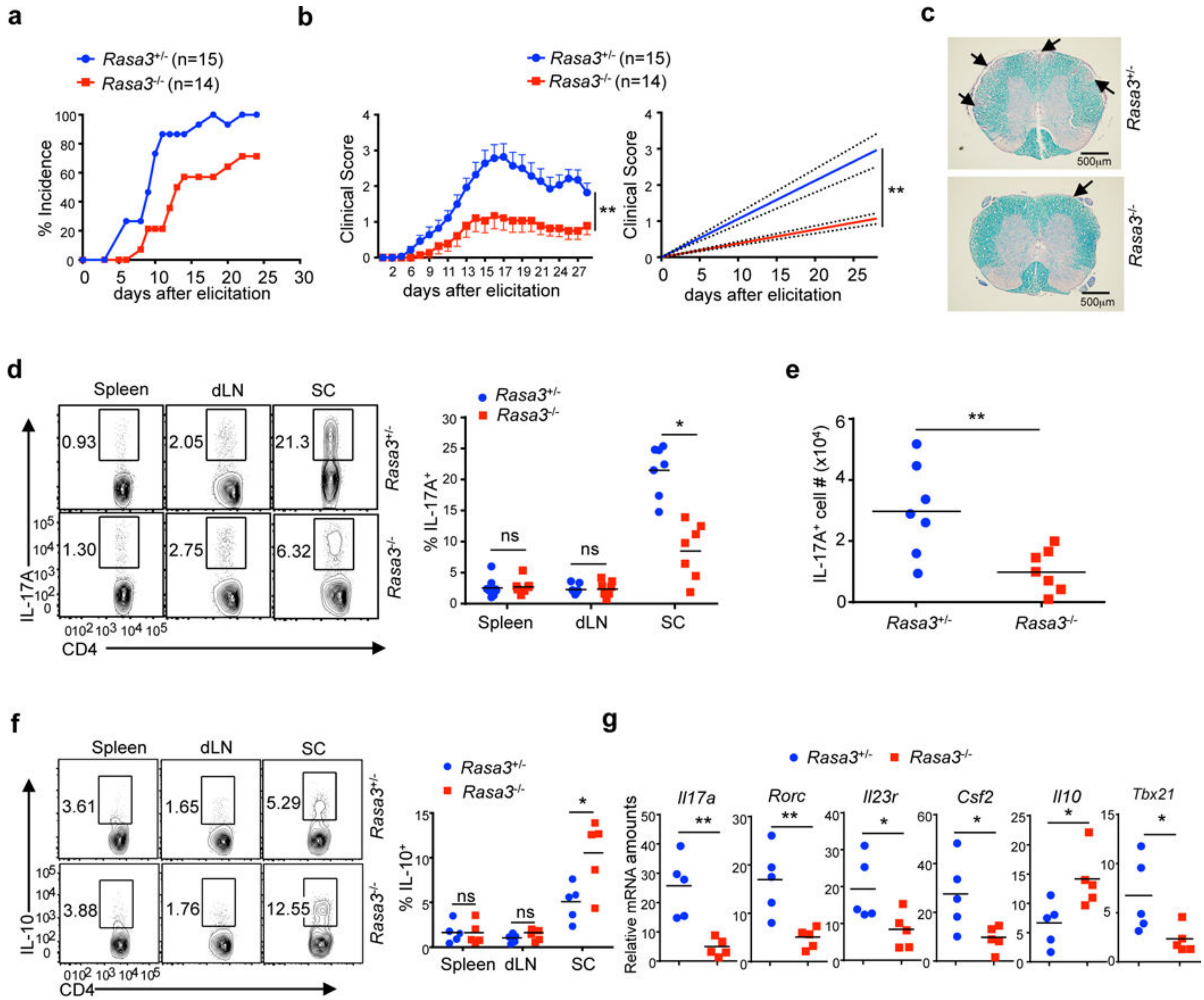

**Figure 2. RASA3 is central to the immune-pathology and pTh17 cell generation during MOG-CFA-elicited EAE.**

(**a-b**) The disease incidence (**a**) and the recorded clinical scores (**b**, left panel) and the linear-regression analysis (**b**, right panel) of mice of indicated genotypes at different time points after EAE elicitation. (The numbers (n) of mice used for each group are from 3 independent experiments. mean ± s.e.m.; **p<0.01 per Mann-Whitney test)

(**c**) Pathology in the spinal cords of diseased mice of indicated genotypes. Results are representative of 3 independent experiments.

(**d-e**) The percentages (**d**) and numbers (**e**) of IL-17A-producing $CD4^+$ T cells in the spleens, draining lymph-nodes (dLN) and spinal cords (SC) of diseased mice of indicated genotypes, assessed by flow-cytometry. (n=7 mice from 3 independent experiments, ns, not significant, *p<0.01, **p<0.01, per two-sided *t*-test; centers indicate the mean values)

(**f**) Flow cytometry of $IL\text{-}10^+$ $CD4^+$ T cells in the spleen, draining lymph-nodes (dLN) and spinal cords (SC) of diseased mice of indicated genotypes. (n=5 mice from 3 independent experiments; ns, not significant, *p<0.01, per two-sided *t*-test; centers indicate the mean values)

(**g**) mRNA levels of Th17-related genes in spinal-cord-infiltrating $CD4^+$ T cells isolated from diseased mice of indicated genotypes, assayed by qRT-PCR. (n=5 mice from 3 independent experiments; *p<0.01, **p<0.01, per two-sided *t*-test; centers indicate the mean values)

See also Figure S2.

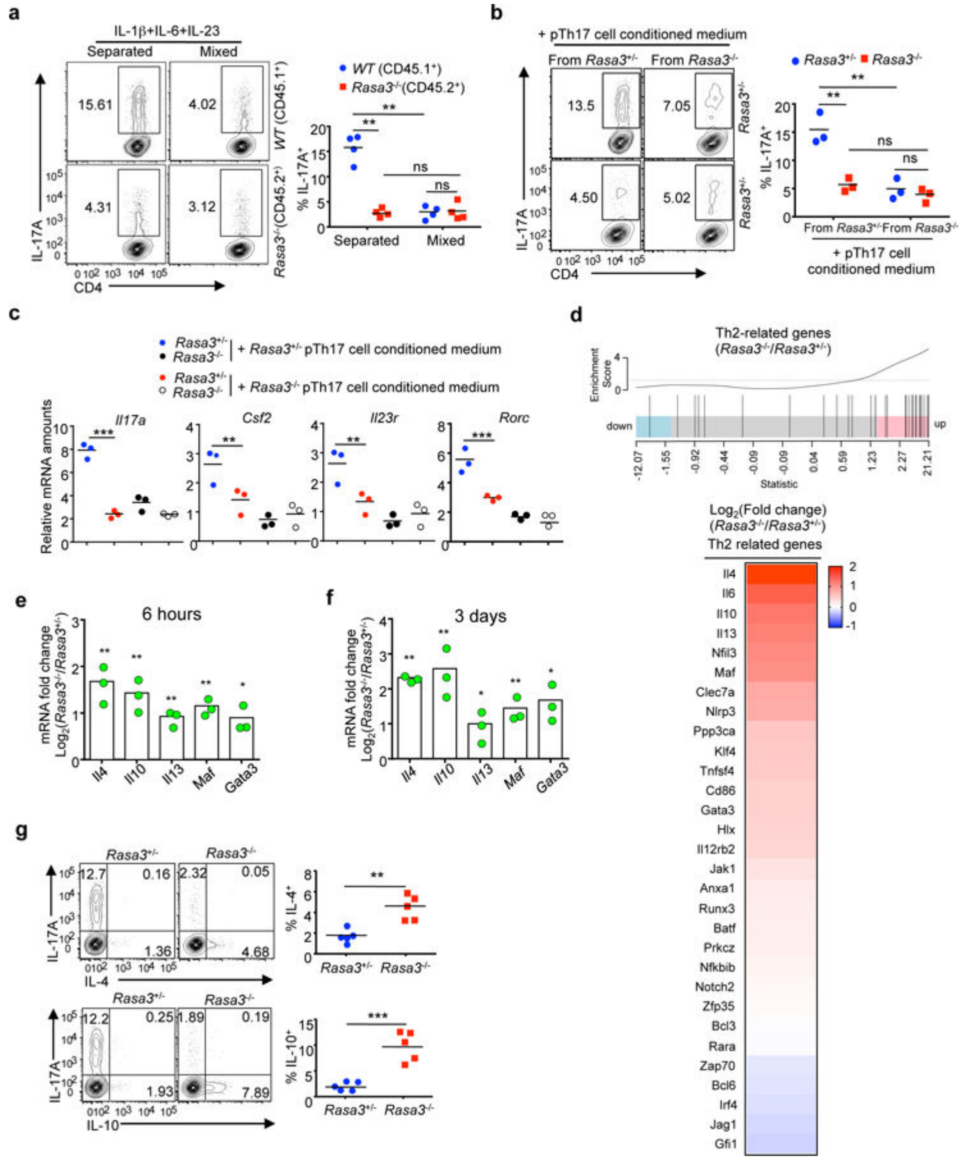


**Figure 3. RASA3-deficient CD4⁺ T cells dominantly trans-repress pTh17 cellgeneration via soluble factors of Th2-bias.**

(**a**) Flow-cytometry of IL-17A production by CD4$^+$ T cells isolated from wild-type (CD45.1$^+$) and *Rasa3*$^{flox/flox}$*Cd4Cre* (CD45.2$^+$, *Rasa3*$^{-/-}$) mice, 4 days after activated either separately or mixed at the ratio of 1:1 under pTh17 cell polarizing condition. (n=4 samples from 4 independent experiments; ns, not significant, **p<0.01, per two-sided *t*-test; centers indicate the mean values)

(**b**) Flow cytometry of IL-17A production by CD4$^+$ T cells of indicated genotypes, 4 days after activated in the conditioned media extracted from *Rasa3*$^{flox/+}$*Cd4Cre* (*Rasa3*$^{+/-}$) or *Rasa3*$^{flox/flox}$*Cd4Cre* (*Rasa3*$^{-/-}$) pTh17 cell cultures. (n=3 samples from 3 independent experiments; ns, not significant, **p<0.01, per two-sided *t*-test; centers indicate the mean values) (**c**) mRNA levels of Th17-related genes in cells as described in (**b**), assayed by qRT-PCR. (n=3 samples from 3 independent experiments; **p<0.01; ***p<0.001, per two-sided *t*-test; centers indicate the mean values)

(**d**) Barcode plots, the enrichment scores and empirical t test statistics of Th2-related genes (as black bars in top panel) and the differential expression of Th2-related genes (lower panel) by *Rasa3*$^{flox/flox}$*Cd4Cre* (*Rasa3*$^{-/-}$) versus *Rasa3*$^{flox/+}$*Cd4Cre* (*Rasa3*$^{+/-}$) $CD4^+$ T cells, 6 hours after activated under pTh17 cell polarizing condition, assayed by RNA-seq. (results are averages of two independent experiments)

(**e-f**) Fold differences of the mRNA expression of Th2-related genes in RASA3 knockout *Rasa3*$^{flox/flox}$*Cd4Cre* (*Rasa3*$^{-/-}$) vs. *Rasa3*$^{flox/+}$*Cd4Cre* (*Rasa3*$^{+/-}$) $CD4^+$ T cells, after activated under pTh17 cell polarizing condition for 6 hours (**e**) and 3 days (**f**), assayed by qRT-PCR. (n=3 samples from 3 independent experiments, *p<0.05; **p<0.01, per two-sided *t*-test; bars indicate the mean values)

(**g**) Flow cytometry of IL-4 and IL-10 production by $CD4^+$ T cells of indicated genotypes, 4 days after activated under pTh17 cell polarizing condition. (n=5 samples from 5 independent experiments; **p<0.01 ***p<0.001, per two-sided *t*-test; centers indicate the mean values) See also Figure S3.

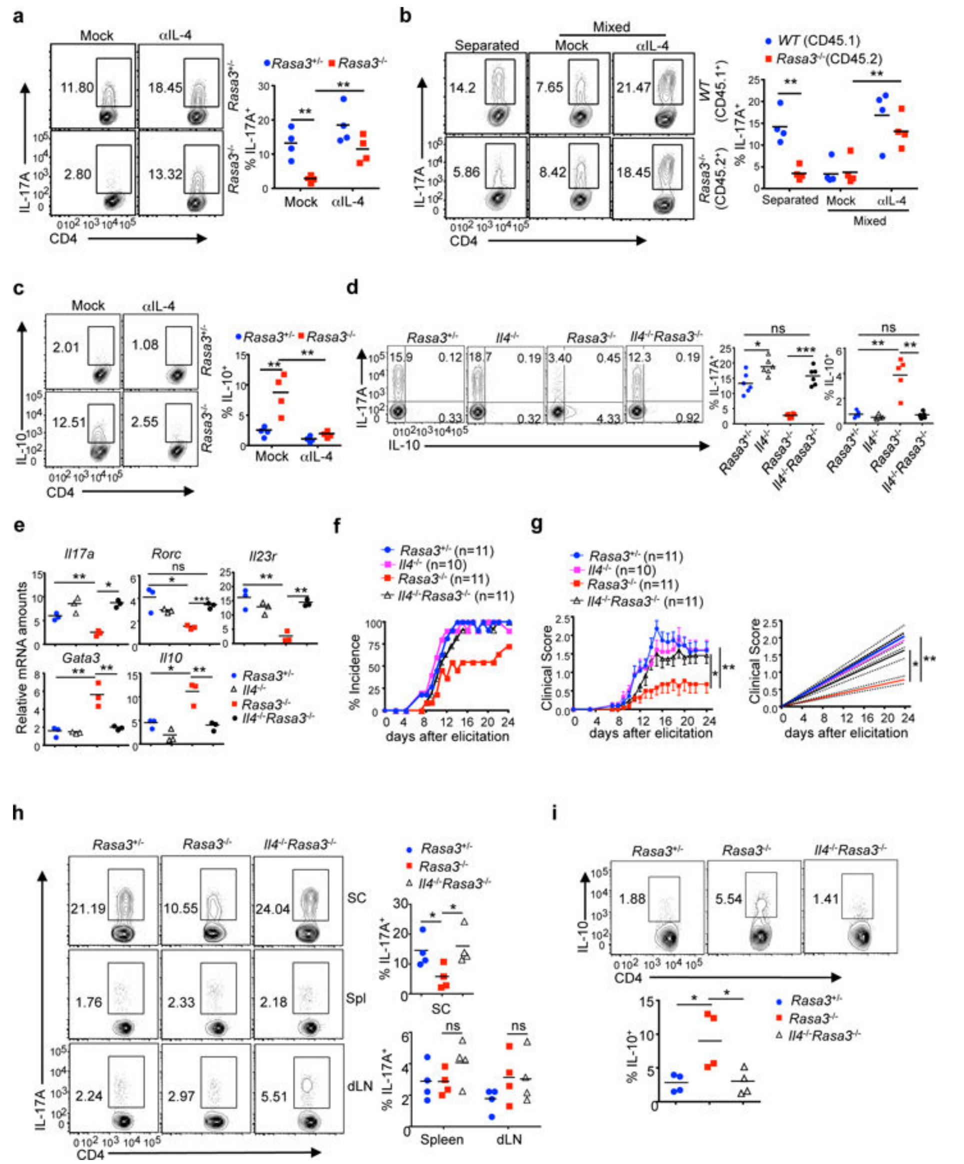

**Figure 4. Aberrant IL-4 expression leads to defective pTh17 generation of RASA3-deficient T cells.**

(**a**) Flow-cytometry to assess the effect of IL-4 neutralization (0.04μg/ml αIL-4) on IL-17A production by *Rasa3*$^{flox/flox}$*Cd4Cre* (*Rasa3*$^{-/-}$) and *Rasa3*$^{flox/+}$*Cd4Cre* (*Rasa3*$^{+/-}$) CD4$^{+}$ T cells activated under pTh17 cell polarizing condition. (n=4 samples from 4 independent experiments; **p<0.01 per two-sided *t*-test; centers indicate the mean values)

(**b**) Flow-cytometry to assess the effect of IL-4 neutralization (0.04μg/ml αIL-4) on *Rasa3*$^{flox/flox}$*Cd4Cre* (*Rasa3*$^{-/-}$, CD45.2$^{+}$) CD4$^{+}$ T cell-mediated trans-suppression of wild-type (CD45.1$^{+}$) pTh17 cell generation (as described in Figure 3a). (n=4 samples from 4 independent experiments; **p<0.01, per two-sided *t*-test; centers indicate the mean values)

(**c**) Flow cytometry to assess the effect of IL-4 neutralization (using 0.04μg/ml αIL-4) on IL-10 production by *Rasa3*$^{flox/flox}$*Cd4Cre* (*Rasa3*$^{-/-}$) and *Rasa3*$^{flox/+}$*Cd4Cre* (*Rasa3*$^{+/-}$)CD4$^{+}$ T cells activated under pTh17 cell polarizing condition. (n=4 samples from 4 independent experiments; **p<0.01 per two-sided *t*-test; centers indicate the mean values) (**d**) Flow-cytometry to compare IL-17A production by *Rasa3*$^{flox/+}$*Cd4Cre* (*Rasa3*$^{+/-}$), IL-4deficient (*Il4*$^{-/-}$), *Rasa3*$^{-/-}$ and *Il4*$^{-/-}$*Rasa3*$^{flox/flox}$*Cd4Cre* (*Il4*$^{-/-}$*Rasa3*$^{-/-}$) CD4$^{+}$ T cells activated under pTh17 cell polarizing condition. (n=6 samples from 3 independent experiments; ns, not significant, *p<0.05, **p<0.01, ***p<0.001, per two-sided *t*-test; centers indicate the mean values)

(**e**) qRT-PCR assay to compare the mRNA levels of Th17- and Th2-related genes inCD4$^{+}$ T cell of indicated genotypes, 4 days after activated under pTh17 cell polarizing condition. (n=3 samples from 3 independent experiments; ns, not significant, *p<0.05, **p<0.01, per two-sided *t*-test; centers indicate the mean values)

(**f-g**) The disease incidence (**f**) and the recorded clinical scores (**g**, left panel) and the linear-regression analysis (**g**, right panel) of mice of indicated genotypes at different time points after EAE elicitation. (The numbers (n) of mice used for each group are from 3 independent experiments. mean ± s.e.m.; *p<0.05, **P<0.01 per Mann-Whitney test)

(**h**) Flow-cytometry of IL-17A produced by CD4$^{+}$ T cells in the spleens, draining lymph-nodes (dLN) and spinal cords (SC) of diseased mice of indicated genotypes, assessed by flow-cytometry. (n=4 mice from 2 independent experiments, ns, not significant, *p<0.01, per two-sided *t*-test; centers indicate the mean values)

(**i**) Flow cytometry of IL-10 produced by CD4$^{+}$ T cells in the spinal cords of diseased mice of indicated genotypes. (n=4 mice from 2 independent experiments; *p<0.01 per two-sided *t*-test; centers indicate the mean values)

See also Figure S4.

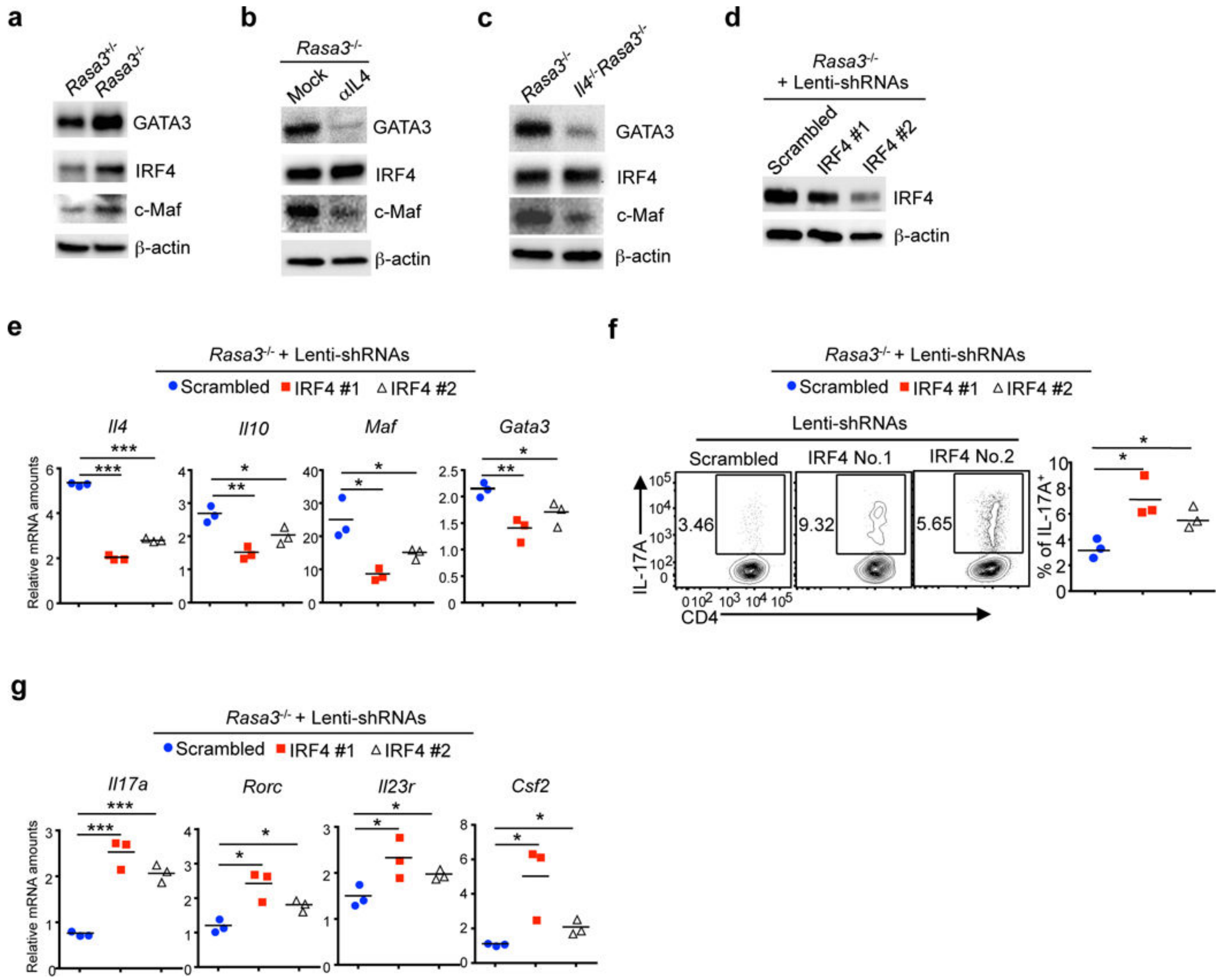

**Figure 5. RASA3 controls IL-4 expression in pTh17 cells via IRF4.**

**(a-b)** Immuno-blotting of GATA3, IRF4 and c-Maf in the *Rasa3*$^{flox/+}$*Cd4Cre* (*Rasa3*$^{+/-}$)and *Rasa3*$^{flox/flox}$*Cd4Cre* (*Rasa3*$^{-/-}$) CD4$^{+}$ T cells activated for 1 day under pTh17 cell polarizing condition, without (**a**) or with IL-4 neutralizing antibody (**b**) as indicated. Results are representative of 3 independent experiments.

(**c**) Immuno-blotting of GATA3, IRF4 and MAF in the *Rasa3*$^{flox/flox}$*Cd4Cre* (*Rasa3*$^{-/-}$) and *Il4*$^{-/-}$*Rasa3*$^{flox/flox}$*Cd4Cre* (*Il4*$^{-/-}$*Rasa3*$^{-/-}$) CD4$^{+}$ T cells activated for 1 day under pTh17 cell polarizing condition. Results are representative of 3 independent experiments.

(**d**) Immuno-blotting to assess IRF4 knockdown efficiency by lentiviral-based shRNAs in *Rasa3*$^{flox/flox}$*Cd4Cre* (*Rasa3*$^{-/-}$) CD4$^{+}$ T cells activated for 5 days under pTh17 cell polarizing condition. Results are representative of 3 independent experiments.

**(e)** qRT-PCR assays to determine mRNA levels of Th2-related genes expressed in cells as described in **d**. (n=3 samples from 3 independent experiments; *p<0.05, **p<0.01, ***p<0.001 per two-sided *t*-test; centers indicate the mean values)

**(f)** Flow-cytometry of IL-17A produced by cells as described in (**d**). (n=3 samples from 3 independent experiments, *p<0.05 per two-sided *t*-test; centers indicate the mean values)
**(g)** qRT-PCR assays to determine mRNA levels of Th17-related genes expressed in cells as described in (**d**). (n=3 samples from 3 independent experiments; *p<0.05, ***p<0.001, per two-sided *t*-test; centers indicate the mean values)
See also Figure S5.

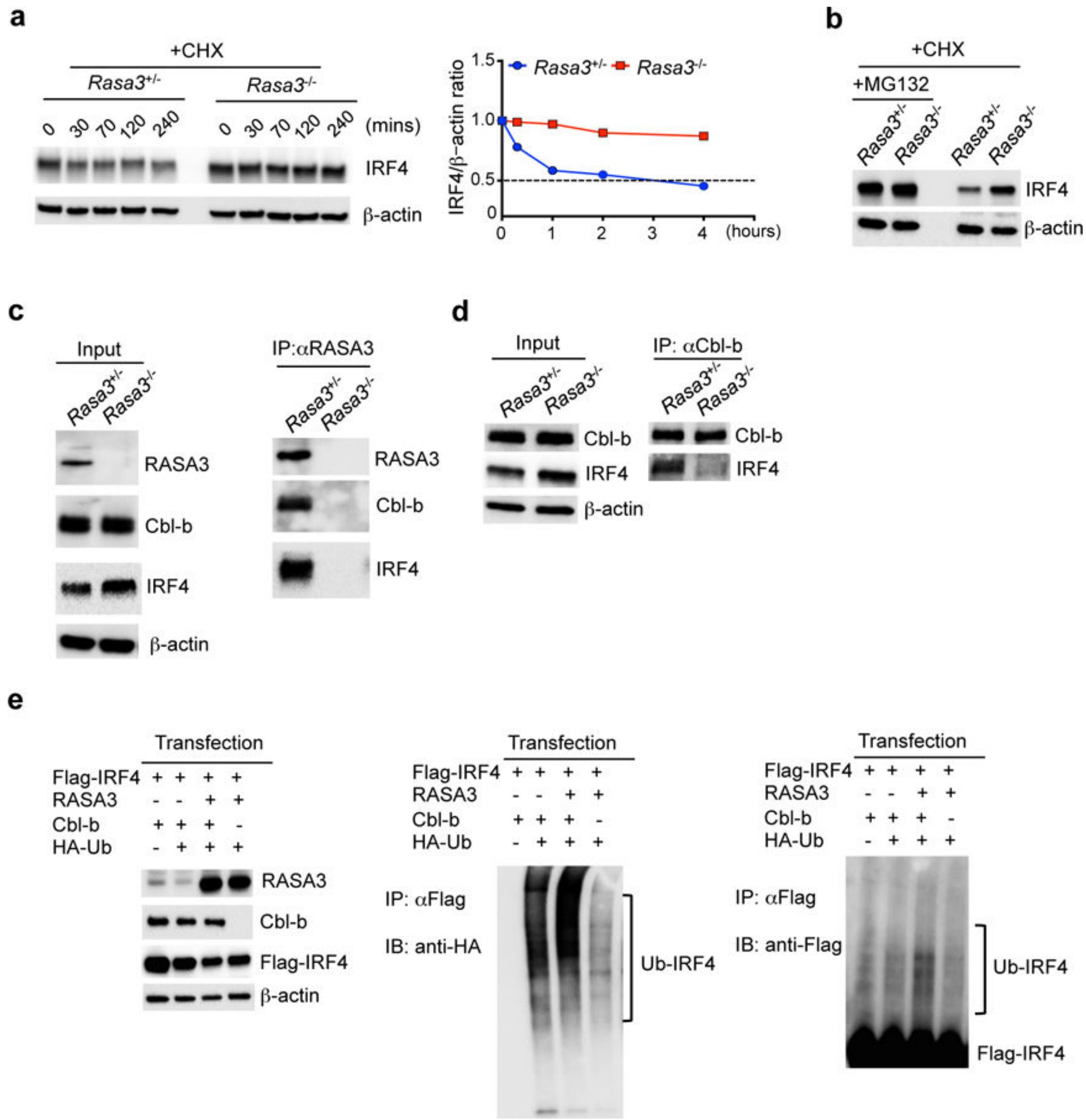


**Figure 6. RASA3 bridges the interaction between Cbl-b and IRF4 to promote IRF4 degradation.**

(**a**) Immuno-blotting of IRF4 in *Rasa3*$^{flox/+}$*Cd4Cre* (*Rasa3*$^{+/-}$) and *Rasa3*$^{flox/flox}$*Cd4Cre* (*Rasa3*$^{-/-}$) CD4$^{+}$ T cells activated for 1 day under pTh17 cell polarizing condition, after treating with translation inhibitor cycloheximide (CHX) for indicated time to determine IRF4 protein half-life. Results are representative of 3 independent experiments.

(**b**) Immuno-blotting of IRF4 in *Rasa3*$^{flox/+}$*Cd4Cre* (*Rasa3*$^{+/-}$) and *Rasa3*$^{flox/flox}$*Cd4Cre* (*Rasa3*$^{-/-}$) CD4$^{+}$ T cells activated for 1 day under pTh17 cell polarizing condition, after treating with translation inhibitor CHX and proteasome inhibitor MIG132 for 4 hours as indicated. Results are representative of 3 independent experiments.

(**c**) The interactions between RASA3 with Cbl-b and IRF4, detected by co-immuno-precipitation in *Rasa3*$^{flox/+}$*Cd4Cre* (*Rasa3*$^{+/-}$) and *Rasa3*$^{flox/flox}$*Cd4Cre* (*Rasa3*$^{-/-}$) CD4$^{+}$ T cells activated for 1 day under pTh17 cell polarizing condition. Results are representative of 3 independent experiments.

(**d**) The interaction between Cbl-b and IRF4, detected by co-immuno-precipitation in *Rasa3*$^{flox/+}$*Cd4Cre* (*Rasa3*$^{+/−}$) and *Rasa3*$^{flox/flox}$*Cd4Cre* (*Rasa3*$^{−/−}$) $CD4^+$ T cells activated for 1 day under pTh17 cell polarizing condition. Results are representative of 3 independent experiments.

(**e**) 293T cells were transfected with plasmids encoding Flag-IRF4, Cbl-b, RASA3 and HA-Ub (ubiquitin) as indicated. The protein levels of IRF4, Cbl-b and RASA3 were determined by immuno-blotting. The poly-ubiquitination of IRF4 was detected through Flag-IRF4 immuno-precipitation followed by immuno-blotting for HA-Ub and Flag. Results are representative of 3 independent experiments.

See also Figure S6.

| REAGENT or RESOURCE | SOURCE | IDENTIFIER |
|---|---|---|
| **Antibodies** | | |
| Pacific Blue anti-mouse CD4 | Biolegend | Cat# 100531<br>RRID:AB_493646 |
| FITC anti-mouse CD8α | Biolegend | Cat# 100706<br>RRID:AB_312744 |
| Percp/Cy5.5 anti-mouse CD4 | Biolegend | Cat# 100434<br>RRID:AB_893324 |
| PE anti-mouse CD25 | eBioscience | Cat# 12–0251-82<br>RRID:AB_465607 |
| FITC anti-mouse CD44 | eBioscience | Cat# 11–0441-82RRID:AB_465045 |
| APC anti-mouse CD62L | eBioscience | Cat# 17–0621-82RRID:AB_469410 |
| APC anti-mouse Foxp3 | eBioscience | Cat# 17–5773-82RRID:AB_469457 |
| PE anti-mouse IL-10 | eBioscience | Cat# 12–7101-82RRID:AB_466176 |
| APC anti-mouse IL-17A | Biolegend | Cat# 506916<br>RRID:AB_536018 |
| PE anti-mouse IL-17A | Biolegend | Cat# 506904<br>RRID:AB_315464 |
| FITC anti-mouse CD45.2 | Biolegend | Cat# 109806<br>RRID:AB_313443 |
| PE anti-mouse IL-4 | Biolegend | Cat# 504104<br>RRID:AB_315318 |
| APC anti-mouse IL-4 | Biolegend | Cat# 504106<br>RRID:AB_315320 |
| FITC anti-mouse IFN-γ | Biolegend | Cat# 505806<br>RRID:AB_315400 |
| PE anti-mouse IFN-γ | Biolegend | Cat# 505808<br>RRID:AB_315402 |
| 7-AAD (7-Aminoactinomycin D) | BD Bioscience | Cat# 559925 |
| PE anti-Annexin V | BD Bioscience | Cat# 556422 |
| Anti-mouse GATA3 | BD Bioscience | Cat# 558686<br>RRID:AB_2108590 |
| Anti-mouse c-Maf | Proteintech Group | Cat# 55013-AP<br>RRID:AB_10863127 |
| Anti-mouse RASA3 | Provided by Dr. Wolfgang Bergmeier | N/A |
| Anti-Flag M2 | Sigma | Cat# F3165<br>RRID:AB_259529 |
| Anti-HA-HRP | Sigma | Cat# H-6533<br>RRID:AB_439705 |
| Anti-mouse Cbl-b | Santa Cruz | Cat# SC-8006<br>RRID:AB_626816 |
| Anti-mouse β-actin | Santa Cruz | Cat# SC-1616<br>RRID:AB_630836 |

| REAGENT or RESOURCE | SOURCE | IDENTIFIER |
|---|---|---|
| Anti-mouse BATF | Santa Cruz | Cat# SC-100974RRID:AB_1119410 |
| Anti-mouse Phospho-STAT3 | Cell Signal Technology | Cat# 9145RRID:AB_2491009 |
| Anti-mouse STAT3 | Cell Signal Technology | Cat# 4904RRID:AB_331269 |
| Anti-mouse Phospho-STAT6 | Cell Signal Technology | Cat# 9361RRID:AB_331595 |
| Anti-mouse STAT6 | Cell Signal Technology | Cat# 9362RRID:AB_2271211 |
| Anti-mouse IRF4 | Cell Signal Technology | Cat# 15106 |
| *InVivo*MAb anti-mouse IFN-γ | BioXcell | Cat# BE0055, RRID:AB_1107694 |
| *InVivo*MAb anti-mouse IL-4 | BioXcell | Cat# BE0045, RRID:AB_1107707 |
| *InVivo*MAb anti-mouse IL-10 | BioXcell | Cat# BE0049, RRID:AB_1107696 |
| **Biological Samples** | | |
| Fetal Bovine Serum | Corning | Cat# 35–015-CV |
| **Chemicals, Peptides, and Recombinant Proteins** | | |
| PBS (Phosphate buffered saline) | Homemade | N/A |
| CD4 (L3T4) MicroBeads, mouse | Miltenyi Biotec | Cat# 130–117-043 RRID:AB_2722753 |
| Collagenase D | Sigma | Cat# 11088866001 |
| Percoll | Sigma | Cat# P-4937 |
| Anti-FLAG® M2 Magnetic Beads | Sigma | Cat# M8823 RRID:AB_2637089 |
| Surebeads™ Protein A magnetic beads | Bio-Rad | Cat# 1614013 |
| Surebeads™ Protein G magnetic beads | Bio-Rad | Cat# 1614023 |
| Laemmli sample buffer | Bio-Rad | Cat# 161–0737 |
| Liberase TL | Roche | Cat# 05401020001 |
| DNase I | Roche | Cat# 11284932001 |
| RPMI 1640 | Gibco | Cat# 32404–014 |
| HEPES buffer | Gibco | Cat# 15630080 |
| Foxp3 / Transcription Factor Staining Buffer Set | eBioscience | Cat# 00–5523-00 |
| Fixation/Permeabilization Solution Kit | BD Bioscience | Cat# 554714 |
| Triton X-100 | Sigma | Cat# T-8787 |
| DTT, 1,4-Dithiothreitol | Sigma | Cat# 10197777001 |
| Nonidet™ P 40 Substitute | Sigma | Cat# 74385 |
| Incomplete Freund's adjuvant | Difco Laboratories | Cat# BD™ 263910 |

| REAGENT or RESOURCE | SOURCE | IDENTIFIER |
|---|---|---|
| *Mycobacterium tuberculosis* H37RA | Difco Laboratories | Cat# BD™ 231141 |
| Murine myelin oligodendrocyte glycoprotein (MOG) peptide 35–55 | AnaSpec | Cat# AS-60130–1 |
| carboxyfluorescein diacetate succinimidyl ester (CFSE) | AnaSpec | Cat# AS-89000 |
| X-VIVO 20 medium | Lonza | Cat# 04–448QT |
| Puromycin | ThermoFisher | Cat# A1113802 |
| Polybrene A | abm | Cat# G-062 |
| Pertussis toxin | List Biological | Cat# 180 |
| Recombination IL-1β | Biolegend | Cat# 575106 |
| Recombination mIL-4 | Biolegend | Cat# 574304 |
| Recombination mIL-6 | Biolegend | Cat# 575706 |
| Recombination mIL-12 | Biolegend | Cat# 577004 |
| Recombination IL-23 | Biolegend | Cat# 589006 |
| Recombination TGF-β | Biolegend | Cat# 580704 |
| **Critical Commercial Assays** | | |
| RNeasy mini kit | Qiagen | Cat# 74104 |
| TruSeq RNA Sample Prep Kit | Illumina | Cat# RS-122–2001 |
| **Deposited Data** | | |
| RNA sequencing data | This Paper | GSE111473 |
| **Experimental Models: Cell Lines** | | |
| HEK293T cells | ATCC | Cat# CRL-3216, RRID:CVCL_0063 |
| **Experimental Models: Organisms/Strains** | | |
| Mouse: B6.SJL-PtprcaPepcb/BoyCrl | Charles River | Cat# CRL:494, RRID:IMSR_CRL:494 |
| Mouse: B6.Cg-Tg(Cd4-cre)1Cwi/BfluJ | The Jackson Laboratory | Cat# JAX:022071, RRID:IMSR_JAX:022071 |
| Mouse: *Rasa3*$^{flox/flox}$ (Rasa3$^{tm1.1Wber}$) | From Dr. Wolfgang Bergmeier | L Stefanini et al; 2015 MGI:5756029 |
| Mouse: *Il4*$^{-/-}$ (B6.129P2-Il4<tm1Cgn>/J) | The Jackson Laboratory | Cat# Jax002253 RRID:IMSR_JAX:002253 |
| **Oligonucleotides** | | |
| **Recombinant DNA** | | |
| RASA3 cDNA | Transomic | Cat# BC068297 |
| IRF4 cDNA | Transomic | Cat# BC137713 |
| Cbl-b cDNA | Transomic | Cat# BC150934 |
| MSCV-IRES-EGFP (MIG) | Addgene | Cat# 20672 |
| MSCV-IRES-Thy1.1 (MIT) | Addgene | Cat# 17442 |
| pCMV-HA-Ub | Addgene | Cat# 18712 |
| pLKO.1-scramble shRNA control | Addgene | Cat# 10878 |

| REAGENT or RESOURCE | SOURCE | IDENTIFIER |
|---|---|---|
| Flag-IRF4 | This paper | N/A |
| MIT-IRF4 | This paper | N/A |
| IRF4 shRNA clone #1 | Sigma | Cat# TRCN0000081550 |
| IRF4 shRNA clone #2 | Sigma | Cat# TRCN0000081552 |
| **Software and Algorithms** | | |
| Diva | BD Biosciences | http://www.bdbiosciences.com/us/instruments/clinical/software |
| FlowJo, v7.0 | FlowJo, Treestar Inc. | https://www.flowjo.com;RRID:SCR_008520 |
| MaxQuant software version 1.6.0.16 | (Max Planck Institute, Germany) | http://www.coxdocs.org/doku.php?id=maxquant:common:download_and_installation |
| Perseus (Version 1.6.0.7) | Perseus Documention | http://www.perseus-framework.org;RRID:SCR_015753 |
| PRISM, v7 | GraphPad Software | https://www.graphpad.com/scientific-software/prism/;RRID:SCR_002798 |
| Salmon, version 0.9.1 | Patro et al., 2017 | N/A |
| R packages in Bioconductor, tximport and tximportData | Soneson et al., 2015 | N/A |
| R function voom | Law et al., 2014 | N/A |
| R function CAMERA | Wu and Smyth, 2012 | N/A |
| **Other** | | |
| EASY-Spray C18 Column | Thermo Fisher | Cat# ES802 |